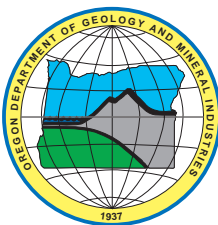


State of Oregon
Department of Geology and Mineral Industries
Vicki S. McConnell, State Geologist

**Interpretive Map Series
IMS-25**

**TSUNAMI HAZARD MAP OF THE FLORENCE-SIUSLAW RIVER AREA,
LANE COUNTY, OREGON**

By
George R. Priest¹, Arun Chawla², and Jonathan C. Allan¹



2007

¹Oregon Department of Geology and Mineral Industries, Coastal Field Office, 313 SW 2nd Street, Suite D, Newport, Oregon 97365

²Center for Coastal and Land-Margin Research, Oregon Graduate Institute School of Science and Engineering,
Oregon Health and Science University, 20000 NW Walker Road, Beaverton, Oregon 97006

NOTE:

The Oregon Department of Geology and Mineral Industries is publishing this map because the subject matter is consistent with the mission of the Department. The map is not intended to be used for site specific planning. It may be used as a general guide for emergency response planning.

Publication IMS-25
Oregon Department of Geology and Mineral Industries
Published in conformance with ORS 516.030

For copies of this publication or other information about Oregon's geology and natural resources, contact:

Nature of the Northwest Information Center
800 NE Oregon Street #5
Portland, Oregon 97232
(503) 872-2750
<http://www.naturenw.org>

or these DOGAMI field offices:

Baker City Field Office
1510 Campbell St.
Baker City, OR 97814-3442
Telephone (541) 523-3133
Fax (541) 523-5992

Grants Pass Field Office
5375 Monument Drive
Grants Pass, OR 97526
Telephone (541) 476-2496
Fax (541) 474-3158

For additional information:
Administrative Offices
800 NE Oregon Street, Suite 965
Portland, OR 97232
Telephone (971) 673-1555
Fax (971) 673-1562
<http://www.oregongeology.com>
<http://egov.oregon.gov/DOGAMI/>

TABLE OF CONTENTS

PLATE	iv
INTRODUCTION	1
How to use the accompanying hazard map	1
Evacuation planning	1
EXPLANATION OF MAPPING METHODS AND RESULTS	2
Additional information on mapping and simulation techniques	2
DATA FILES ON THE CD-ROM	4
FUNDING SOURCE	18
ACKNOWLEDGEMENTS	18
REFERENCES	18
APPENDIX 1. REGIONAL TECTONIC DEFORMATION FOR THE SCENARIO EARTHQUAKES	19
APPENDIX 2. ESTIMATED WATER DEPTH FOR THE LARGE-EVENT TSUNAMI FLOODING SCENARIO, 1A + ASPERITY	22
APPENDIX 3. EXPLANATION OF ENERGY COMPENSATION	36
APPENDIX 4. NUMERICAL INSTABILITY IN TSUNAMI SIMULATION 1A	41

LIST OF FIGURES

Figure 1.	Regional extent of tsunami inundation to eastern limit of the numerical simulation	3
Figure 2.	Station 1 (mouth of the Siuslaw River) time history of wave arrivals for three scenario earthquakes on the Cascadia subduction zone fault system	6
Figure 3.	Current velocity changes for station 1 (mouth of the Siuslaw River)	7
Figure 4.	Station 2 time history of wave arrivals	8
Figure 5.	Current velocity changes for station 2	8
Figure 6.	Station 3 time history of wave arrivals	9
Figure 7.	Current velocity changes for station 3	9
Figure 8.	Station 4 time history of wave arrival	10
Figure 9.	Current velocity changes for station 4	10
Figure 10.	Station 5 (northwest Florence) time history of wave arrivals	11
Figure 11.	Current velocity changes for station 5 (northwest Florence)	11
Figure 12.	Station 6 (west Florence) time history of wave arrivals	12
Figure 13.	Current velocity changes for station 6 (west Florence)	12
Figure 14.	Station 7 (south Florence at Highway 101 bridge) time history of wave arrivals	13
Figure 15.	Current velocity changes for station 7 (south Florence at Highway 101 bridge)	13
Figure 16.	Station 8 (southeast Florence east of the Highway 101 bridge) time history of wave arrivals	14
Figure 17.	Current velocity changes for station 8 (southeast Florence east of the Highway 101 bridge)	14
Figure 18.	Station 9 (1 mile east of Florence) time history of wave arrivals	15
Figure 19.	Current velocity changes for station 9 (1 mile east of Florence)	15
Figure 20.	Station 10 (2 miles east of Florence) time history of wave arrivals	16
Figure 21.	Current velocity changes for station 10 (2 miles east of Florence)	16
Figure 22.	Approximate area of assumed foredune erosion for large-event tsunami flooding scenario	17
Figure A1.	Ground deformation for the large-event scenario earthquake (scenario 1A + asperity)	19
Figure A2.	Crustal deformation for the average-event inundation scenario (scenario 1A)	20
Figure A3.	Small-event (smallest) earthquake deformation (scenario 2Cs)	21
Figure A4.	Tsunami water depth contours in feet for the 1A + asperity scenario with mapped inundation and illustration of the 15-m (50 ft) numerical grid used to derive depth contours in populated portions of the Siuslaw Estuary	23
Figure A5.	Downtown Florence (Old Town area)	24
Figure A6.	Florence area on the south side of the Highway 101 bridge	25

LIST OF FIGURES — continued

Figure A7. Florence and adjacent sand spit, immediately northwest of the Old Town area.	26
Figure A8. Northwest Florence between 11th and 1st Avenue West at Riverside Drive	27
Figure A9. Northwest Florence in the vicinity of the local landfill	28
Figure A10. Northwest Florence in the vicinity of 35th and Rhododendron Drive	29
Figure A11. Northwest Florence in the vicinity of the Coast Guard station	30
Figure A12. Mouth of the Siuslaw River in the vicinity of Harbor Vista Park Road	31
Figure A13. Heceta Beach immediately north of the of the Siuslaw River in the vicinity of North Jetty Road to Woodlands Drive.	32
Figure A14. South Heceta Beach in the vicinity of Perpetua and Sebastian Roads	33
Figure A15. Central Heceta Beach from Heceta Beach Road to 2nd Avenue	34
Figure A16. North Heceta Beach from Joshua Lane to Shoreline Loop	35
Figure A17. Energy versus hours of simulation (wave travel time) for the 1A + asperity simulation	37
Figure A18. Comparison of total energy losses before and after adding compensating energy	37
Figure A19. Uplift in meters for the 1A + asperity simulation before and after initial wave elevation is added to compensate for energy losses	38
Figure A20. Comparison in cross section of initial displacement for 1A + asperity scenario before and after elevation is added to compensate for energy losses	38
Figure A21. Location of cross section in Figure A20	39
Figure A22. Large-event (1A + asperity) inundation in downtown Florence with energy compensation and without energy compensation	40
Figure A23. Numerical instability in the 1A simulation generated anomalously high wave elevations.	41
Figure A24. Location of numerical data deleted from the maximum elevation data file 1A__florence.maxelv.txt for the Scenario 1A simulation (average event) to produce file _1A_maxelvNoInstability.txt	42

LIST OF TABLES

Table 1. Tsunami inundation map zone colors and risk for the Florence-Siuslaw River area, Lane county, Oregon	1
Table 2. Oceanographic factors used to predict foredune retreat for the large-event tsunami flooding scenario.	2
Table 3. Digital data files included on the CD-ROM	4

PLATE

Tsunami Hazard Map of the Florence-Siuslaw Area, Lane County, Oregon

INTRODUCTION

The Tsunami Hazard Map of the Florence-Siuslaw River Area, Lane County, Oregon, may be viewed as a guide for evacuation planning in the event of an earthquake and tsunami. The map is not intended to be used for site specific planning. It may be used as a general guide for emergency response planning.

How to use the accompanying hazard map

Mapped boundaries on the accompanying map plate may be viewed as guides for evacuation planning in the event of an earthquake and tsunami. *If strong earthquake shaking lasts 20 seconds or more, go immediately to the lowest risk site available. A tsunami could arrive within a few minutes of the earthquake.* Check the illustrations of estimated tsunami arrival times in this text for an accurate estimate of how much time you have to evacuate after a local earthquake; remember, a local earthquake may shake the ground for several minutes during which time evacuation will not be possible. Such nearby earthquakes and associated tsunamis only occur on the order of 300–600 years. Distant tsunamis (teletsunamis) occur more often, are generally smaller than tsunamis from nearby earthquakes, and arrive hours after a distant earthquake. The West Coast/Alaska Tsunami Warning Center (<http://wcatwc.arh.noaa.gov/main.htm>) issues warnings for all tsunamis affecting the west coast of the United

States; their warnings will be most useful for teletsunamis. Earthquake ground shaking is the best warning for a locally generated tsunami. Remember, wait for the “all clear” from local officials before returning to low lying areas, dangerous tsunami wave activity will continue for several hours and other hazards such as fire and hazardous waste spills could pose a threat.

Evacuation planning

When planning evacuation routes and destinations, check with local officials for guidance. In general, one should go to the least hazardous site on the map (a non-colored area or the coolest color) by the shortest route after making sure that the route is not compromised by other earthquake hazards such as liquefaction or earthquake-induced landslides. Bridges may fail in the event of an earthquake. Consult with transportation authorities about the seismic stability of bridges used for evacuation. Pay particular attention to the time histories of wave arrival (Figures 2 through 21) at the various localities shown in Figure 1. The time to first-wave arrival is the amount of time for evacuation, about 25 minutes at the open coast and about 40 minutes near the Highway 101 bridge at Florence. Note also in Figures 2 through 21 that large waves continue to arrive for several hours after the initial wave.

Table 1. Tsunami inundation map zone colors and risk for the Florence-Siuslaw River area, Lane county, Oregon.

Zone Color	Risk	Notes
White	Low- to negligible-risk zone for tsunami flooding (300-600 year events)	—
Yellow	Moderate-risk zone for tsunami flooding (300-600 year events)	Elevations within and below this zone would be flooded by a Cascadia subduction zone tsunami from a magnitude ~9.1 earthquake with doubling of the fault slip immediately offshore. See Priest and others (1997; 2001 http://www.pmel.noaa.gov/ftp/AD/ryan/gonzalez/R-03_Priest.pdf), model 1A asperity for an explanation of this model earthquake and tsunami. See also Appendix 1.
Orange	High-risk zone for tsunami flooding (300-600 year events)	Elevations within and below this zone would be flooded by a Cascadia subduction zone tsunami from a magnitude ~9.1 earthquake. See Priest and others (1997; 2000; 2001 http://www.pmel.noaa.gov/ftp/AD/ryan/gonzalez/R-03_Priest.pdf), model 1A, for an explanation of this model earthquake and tsunami. See also Appendix 1.
Red	Extreme-risk zone for tsunami flooding (300-600 year events)	Elevations within and below this zone would be flooded by a Cascadia subduction zone tsunami from a magnitude ~8.6 earthquake. See Priest and others (1997; 2000; 2001 http://www.pmel.noaa.gov/ftp/AD/ryan/gonzalez/R-03_Priest.pdf) model 2Cs, for an explanation of this model earthquake and tsunami. See also Appendix 1.

EXPLANATION OF MAPPING METHODS AND RESULTS

Figures 1 through 21 illustrate an overview of the mapped tsunami hazard zones (Figure 1) and the sequence of water elevation and velocity changes from tsunamis arriving after subduction zone earthquakes of three different sizes (Figures 2 through 21). The three scenario tsunamis may be treated as small, average and large flooding events from the Cascadia subduction zone earthquakes (see Priest and others [1997] models 2Cs, 1A, and 1A + asperity for an explanation of scenario earthquakes and tsunamis). Priest and others (1997, 2000 <http://library.lanl.gov/tsunami/ts182.pdf>; 2001 http://www.pmel.noaa.gov/ftp/AD/ryan/gonzalez/R-03_Priest.pdf) summarize fault rupture scenarios 2Cs, 1A, and 1A + asperity used in this investigation. Priest and others (1997) and Myers and others (1999 <http://library.lanl.gov/tsunami/ts182.pdf>) summarize the finite element tsunami simulation technology. Appendix 1 summarizes regional ground deformation predicted for the scenario earthquakes. The undersea portion of this deformation affects the ocean surface, becoming the initial tsunami wave in each scenario. The average- and large-event scenarios predict up to 1 m (3 ft) of subsidence at Florence; the small-event scenario predicts about one third of a meter (one foot) or so of subsidence. View the animations on this CD (files 1Aasp_Florence_elev_anim.gif, 1A_Florence_elev_anim.gif, 2Cs_Florence_elev_anim.gif) to see how the initial tsunami wave travels toward shore and how effectively the offshore submarine bank decreases the wave height for these Cascadia tsunami sources. Appendix 2 illustrates estimates of tsunami water depth for the large-event scenario (scenario 1A + asperity) in the main populated areas of Florence and Heceta Beach. Appendix 2 also illustrates the variation in the density of numerical calculation points (numerical grid) used to simulate tsunami inundation. Appendix 3 summarizes how the initial wave elevations were modified to compensate for energy losses inherent in the numerical technique. Appendix 4 illustrates one area that generated a numerical instability for the scenario 1A (average event) simulation. This instability affected only a small area near the mouth of the estuary and was ignored when generating the hazard map.

Tsunami flooding depicted on the map takes into account current topography with one exception. The large-event flooding scenario (1A + asperity case) assumes that an ocean wave erosion event precedes the tsunami, lowering foredunes to approximately 3.5–3.9

m (11–13 ft) elevation over a width of approximately 60–150 m (200–500 ft) and a length depicted in Figure 22, the width varying with beach slope (lower slope denotes wider). The erosion scenario uses the geometric method of Komar and others (1999) to predict retreat of foredunes assuming a large event.¹ Ocean water levels and other oceanographic factors used in the wave erosion model are summarized in Table 2. Erosion predicted from this scenario effectively removes the entire foredune. Note that the tsunami water depths depicted in Appendix 2 also assume that the foredunes are eroded, so water depths in a real event could be substantially smaller at foredunes relative to those listed in Appendix 2.

Table 2. Oceanographic factors used to predict foredune retreat for the large-event tsunami flooding scenario.

Factor	Value
significant wave height	16.0 m (52.5 ft)
wave period	20-s peak
mean higher high tide	2.3 m (7.55 ft)
monthly mean water level	0.4 m (1.31 ft)
storm surge	1.7 m (5.58 ft)
sea level rise	0.4 m (1.31 ft)

Additional information on mapping and simulation techniques

See Oregon Department of Geology and Mineral Industries (DOGAMI) Open-File Report O-97-34 (Priest and others, 1997) for a detailed explanation of the mapping techniques (to obtain this publication go to World Wide Web site <http://www.oregongeology.com>). The simulation techniques are also discussed by Myers and others (1999) and Priest and others (2000, 2001). World Wide Web links to these references are at <http://library.lanl.gov/tsunami/ts171.pdf>, <http://epubs.lanl.gov/tsunami/ts182.pdf>, and http://www.pmel.noaa.gov/ftp/AD/ryan/gonzalez/R-03_Priest.pdf, respectively.

1. This erosion scenario assumes that the rise in wave heights identified offshore from the Pacific Northwest coast buoy data by Allan and Komar (2000) continues over the next century. In effect, the 16-m (52.5 ft) significant wave height used in this scenario is similar to a predicted 100-yr storm wave. The 0.4-m (1.31 ft) rise in mean sea level is expected to occur over the next 100 years and is based on trends determined for the South Beach, Yaquina Bay tide gauge (Flick and others, 1999). This combination of events has an extremely low probability of occurrence. However, the results are still useful in that they provide a landward limit of potential erosion (assuming no long-term coastal retreat) due to a particularly severe storm.

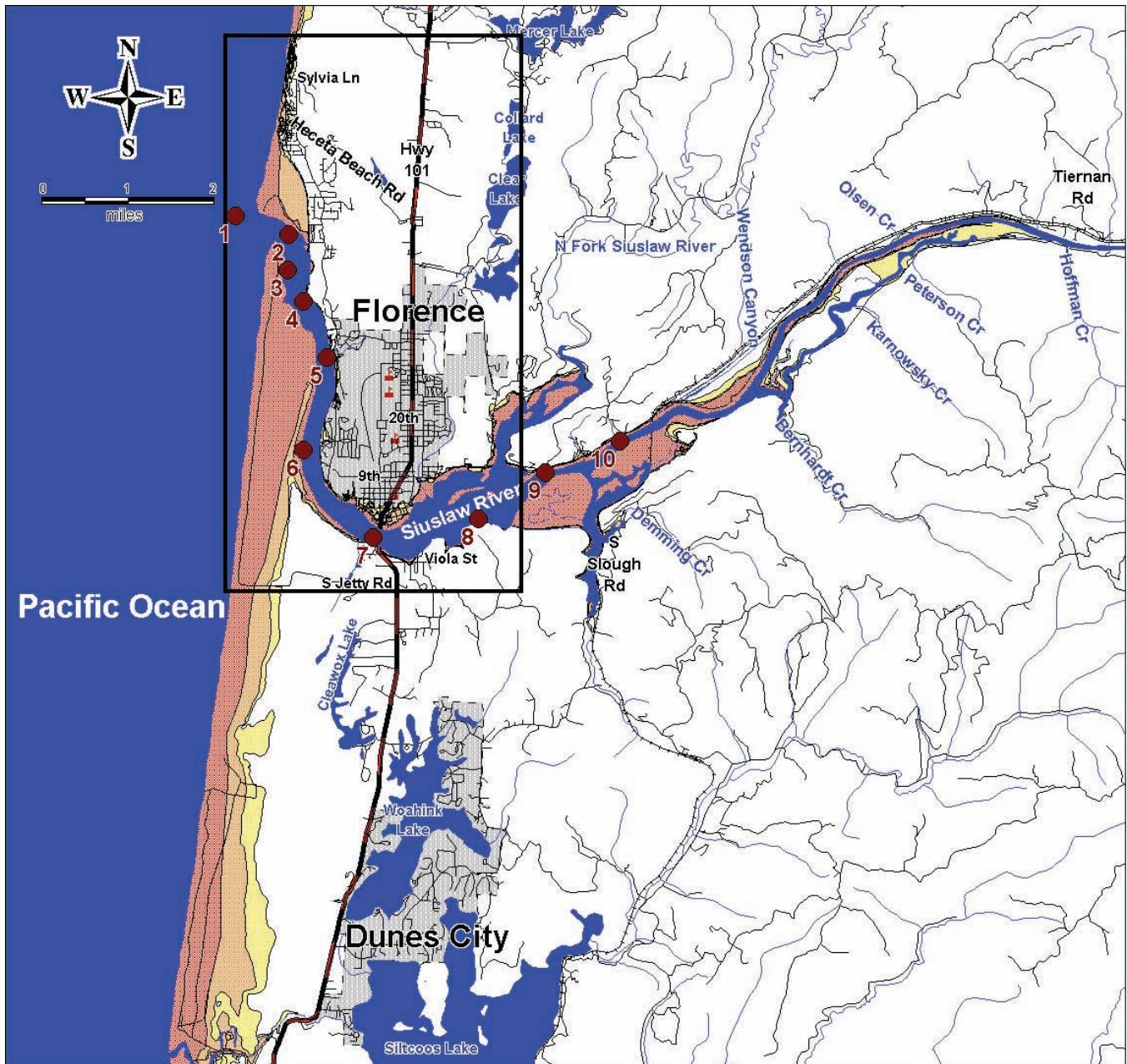


Figure 1. Regional extent of tsunami inundation to eastern limit of the numerical simulation (red is extreme hazard; orange is high hazard; yellow is moderate hazard; and white is low hazard). Boxed area is the mapped area. Map shows locations for 10 observation stations for time histories of tsunami arrivals (reddish-brown numbered dots). Detailed time histories of water elevation (above mean sea level) and velocity (meters per second) for all three scenarios at these observation stations are shown in Figures 2 through 21. Roads and hydrography are from digital files of the Oregon Department of Transportation (<http://www.oregon.gov/ODOT/TD/TDATA/gis/dgnfiles.shtml>).

DATA FILES ON THE CD-ROM

Table 3 lists selected digital data and animation files included on the CD-ROM.

Table 3. Digital data files included on the CD-ROM.

File Name	Description	Metadata Notes
<i>Maximum tsunami wave elevation</i>		
2CS_florence.maxelv.txt	scenario 2Cs	1
1A__florence.maxelv.txt	scenario 1A	1
_1A_maxelvNoInstability.txt	scenario 1A without anomalous data in area with a numerical instability (see explanation in Appendix 4)	1
1Aasp_florence.maxelv.txt	Maximum tsunami wave elevation for scenario 1A + asperity	1
<i>Seafloor deformation</i>		
2Cs_displace_Ecomp2.txt	scenario 2Cs with energy compensation	2
2Cs_displacement.txt	scenario 2Cs without energy compensation	2
1A_displacement_Ecomp.txt	scenario 1A with energy compensation	2
1A_displacement.txt	scenario 1A without energy compensation	2
1Aasp_displace_Ecomp2.txt	scenario 1A + asperity with energy compensation	2
1Aasp_displacement.txt	scenario 1A + asperity without energy compensation	2
<i>Computational bathymetric grid used for numerical calculations</i>		
2Cs_fort14.txt	scenario 2Cs; depths do not have tectonic displacement but do include tide at mean higher high water	3
1A_fort14.txt	scenario 1A; depths do not have tectonic displacement but do include tide at mean higher high water	3
1Aasp_fort14.txt	scenario 1A + asperity; depths do not have tectonic displacement but do include tide at mean higher high water. Digital topography for this scenario includes erosion of coastal foredunes to an elevation of ~3.5–3.9 m.	3

(table continues on next page)

An asterisk denotes a global placeholder for characters in common GIS file extensions for MapInfo or ArcView; GIS is geographic information system; USGS is U.S. Geological Survey; NOAA is National Oceanic and Atmospheric Administration; LIDAR is Light Detection and Ranging data.

Table 3 metadata notes:

1. ASCII format; from left to right data columns are ID number, longitude, latitude, water elevation in meters above mean higher high water (1.28 m [~4 ft] above NGVD29 mean sea level, so computer simulation is run with tide at mean higher high water). To convert water depths to elevations above current geodetic mean sea level NAVD29, add 1.28 m to each point. Map projection is Longitude-Latitude, NAD27, NAVD29 for the continental United States. Negative water depths indicate dry conditions.
2. ASCII format; from left to right data columns are ID number, longitude, latitude, vertical component of coseismic displacement in meters from original state (negative is down; positive is up). This elevation adjustment is made in the water surface elevation in the first few time steps of the simulation and constitutes the initial condition for the tsunami simulation. Map projection is Longitude-Latitude, NAD27 for the continental United States.
3. ASCII format; from left to right data columns are ID number, longitude, latitude, water depth in meters below mean higher high water (MHHW is 1.28 m [~4 ft] above NGVD29 mean sea level, so computer simulation is run with tide at mean higher high water). Negative values are dry land elevations above MHHW. Subtract 1.28 m from each value to get bathymetry without MHHW depth adjustment. Map projection is Longitude-Latitude, NAD27, NAVD29 for the continental United States.

Table 3 — continued

File Name	Description	Metadata Notes
<i>Preliminary data sources</i>		
Siuslaw_bathy_survey.txt	bathymetric survey data (August 25, 2003, to October 31, 2003) for the Siuslaw Estuary	4
Siuslaw_bathlidar.txt	2002 NOAA-USGS LIDAR data used for the simulation	5
Florence_contours.txt	Elevation points in feet along 2-ft (0.6 m) contours from City of Florence topographic survey done in the 1970s	6
SpliceGrid.txt	USGS 10-m digital elevations used for the simulation	7
<i>Tsunami hazard zone polygons</i>		
Instability_II.* (.ID, .MAP)	Polygon (in MapInfo format) where data was deleted from file 1A__florence.maxvel.txt	8
Inundation_ALL_zones.* (.DAT, .ID, .MAP, .TAB)	Tsunami hazard zone polygons in file format for MapInfo GIS software	8
Inundation_ALL_zones*_region.dbf, .prj; shp; .shx	Tsunami hazard zone polygons in file format for ArcView GIS software	9
Inundation_Study_Area* (.DAT, .ID, .MAP, .TAB)	Tsunami hazard zone polygons clipped to the study area boundaries for MapInfo GIS software	8
Inundation_Study_Area* (.dbf, .prj; shp; .shx)	Tsunami hazard zone polygons clipped to the study area boundaries for ArcView GIS software	9
Water_depth_2ft_contours* (.DAT, .ID, .MAP, .TAB)	Tsunami water depth 2-ft (0.6 m) contours for large-event flooding (scenario 1A + asperity) for MapInfo GIS software	8
Water_depth_2ft_contours* (.dbf, .prj; shp; .shx)	Tsunami water depth 2-ft (0.6 m) contours for large-event flooding (scenario 1A + asperity) for ArcView GIS software	9
<i>Maximum tsunami wave velocities</i>		
2Cs__florence.maxvel.txt	scenario 2Cs	10
1A__florence.maxvel.txt	scenario 1A	10
1Aasp_florence.maxvel.txt	scenario 1A + asperity	10

(table continues on next page)

Table 3 metadata notes, continued:

4. ASCII format; from left to right data columns are ID number, longitude, latitude, easting_m, northing_m, and depth in meters and in feet below NGVD29 mean sea level. Map projections are Longitude-Latitude, NAD27 for the continental United States and Universal Transverse Mercator. Bathymetric survey was conducted by Seafloor Systems, Inc., Hillsboro, Oregon.
5. ASCII format; from left to right data columns are ID number, longitude, latitude, land elevation in meters above geodetic mean sea level (NAVD29), NAD27 for the continental United States. Data were downloaded from <http://www.csc.noaa.gov/crs/tcm/missions.html>.
6. ASCII format; from left to right data columns are ID number, longitude, latitude, land elevation in feet above geodetic mean sea level (NAVD29), NAD27 for the continental United States. Data were extracted from topographic contour data provided by the City of Florence.
7. ASCII format; from left to right data columns are ID number, longitude, latitude, land elevation in meters above geodetic mean sea level (NAVD29), NAD27 for the continental United States. Data were downloaded from http://www.reo.gov/reo/data/DEM_Files/indexes/orequadindex.asp.
8. File format for MapInfo GIS software; map projection is Longitude-Latitude, NAD27 for the continental United States.
9. File format for ArcView GIS software; map projection is Oregon Lambert, 1997 feet.
10. ASCII format; from left to right data columns are ID number, longitude, latitude, velocity (meters per second) in "x" direction (west to east is positive), and velocity (meters per second) in "y" direction (south to north is positive). Note that 1 m/s is roughly equal to 2 knots. Map projection is Longitude-Latitude, NAD27 for the continental United States.

Table 3 — continued

File Name	Description	Metadata Notes
<i>Animations</i>		
1Aasp_Florence_elev_anim.gif 1A_Florence_elev_anim.gif, 2Cs_Florence_elev_anim.gif	tsunami inundation (colored contours of elevation) for scenarios 2Cs, 1A, and 1A + asperity; elevations in meters; time in seconds; simulates 4 hours of inundation	—
1Aasp_Florence_velmag_anim.gif 1A_Florence_velmag_anim.gif 2Cs_Florence_velmag_anim.gif	current velocity magnitudes (colored contours) for scenarios 2Cs, 1A, 1A + asperity; velocities in meters per second; time in seconds; simulates 4 hours of inundation	—
1Aasp_Florence_vel_anim.gif 1A_Florence_vel_anim.gif 2Cs_Florence_vel_anim.gif	current velocity vector changes (direction arrows with length proportional to velocity) for scenarios 2Cs, 1A, and 1A + asperity; each animation shows three views: 1) at mouth of the Siuslaw River, 2) in the estuary northwest of downtown Florence, and 3) at the Highway 101 bridge. Each animation has a regional overview of inundation for location purposes; velocities in meters per second; time in seconds; simulates 4 hours of inundation	—

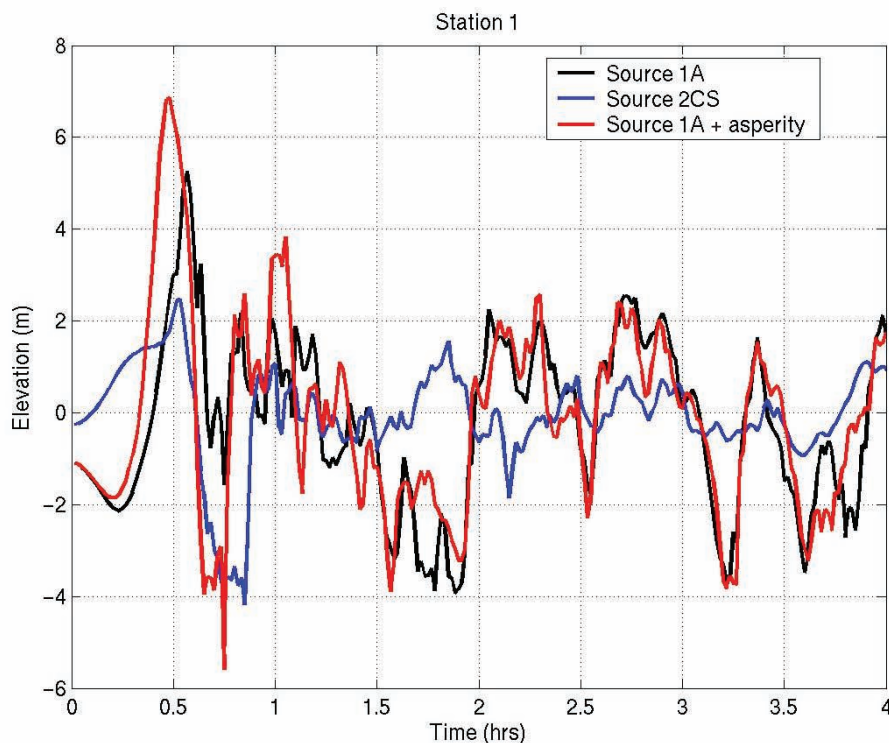


Figure 2. Station 1 time history of wave arrivals for three scenario earthquakes on the Cascadia subduction zone fault system (see station location in Figure 1). Observation point is at the mouth of the Siuslaw River and shows three scenario tsunami simulations, small (2CS), average (1A), and large (1A + asperity) events. Note that a small surge of flooding could occur at the open coast about 15–20 minutes after the earthquake; the main wave arrival at the open coast is at about 25–30 minutes after the earthquake. Minor flooding may occur immediately after the earthquake due to approximately 1 meter of subsidence of the land surface (amount of subsidence is indicated by elevation at 0 hours). Actual tsunami wave elevation at shoreline sites will be higher than shown in the figure, because this simulation was run at mean higher high water (1.28 m above geodetic mean sea level); simulated flood elevation is 1.28 m (4 ft) above the figures shown on the graph. Actual tsunami elevation on adjacent dry land areas during run-up will also differ from this graph. This figure and the ones below should be used to understand approximate timing and relative wave elevation, not absolute wave elevation at the shoreline.

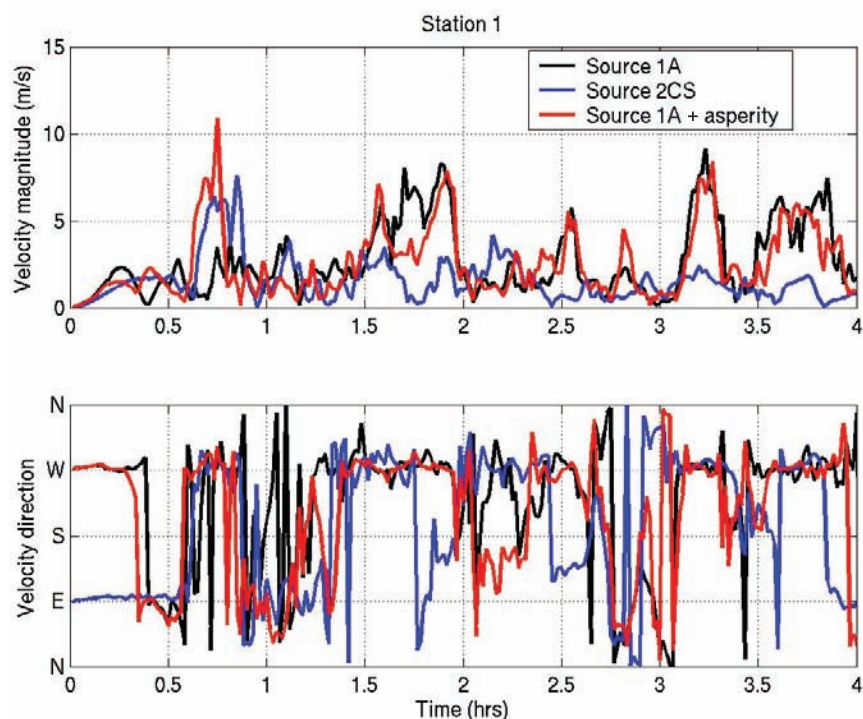


Figure 3. Current velocity changes for station 1 (see station location in Figure 1). Lower graph shows velocity direction changes (N is north; S is south; E is east; W is west). Current direction in the estuary channels could be either seaward (W) or landward (E) during the first 5–10 minutes after the earthquake, depending on how the fault rupture process occurs (e.g., more tectonic subsidence west of observation point than east would yield a withdrawing or seaward current). Note how quickly the current reverses direction as water surges in and out of the estuary. Meters per second converts to knots by multiplying by a factor of about 2, so maximum velocities at this station are on the order of about 15–20 knots during the first 5 hours after the earthquake.

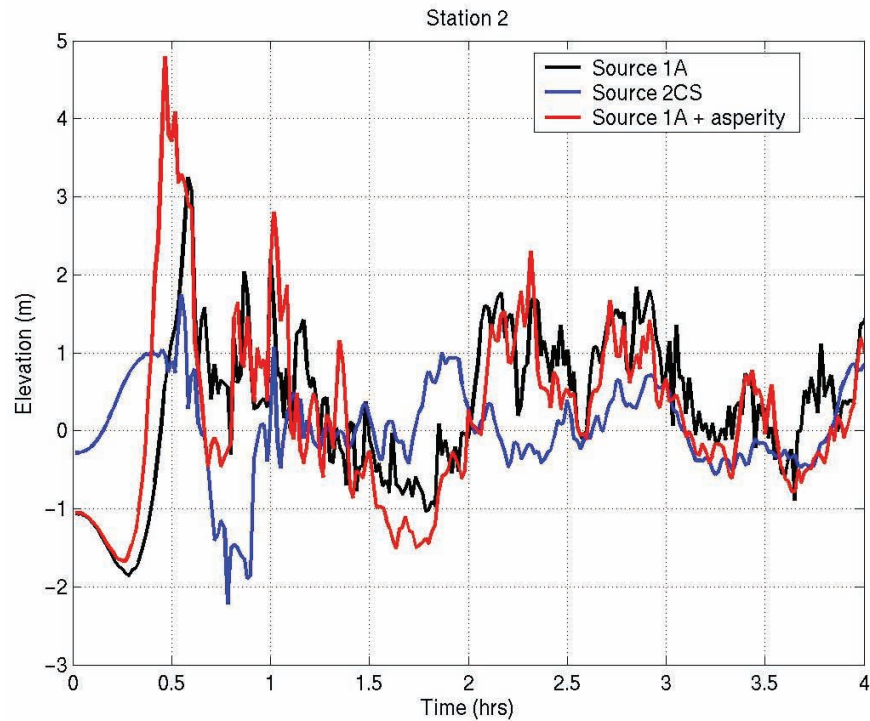


Figure 4. Station 2 time history of wave arrivals; see Figure 1 for station location and Figure 2 caption for general explanation. Note that the first large wave arrives about 20–30 minutes after the earthquake.

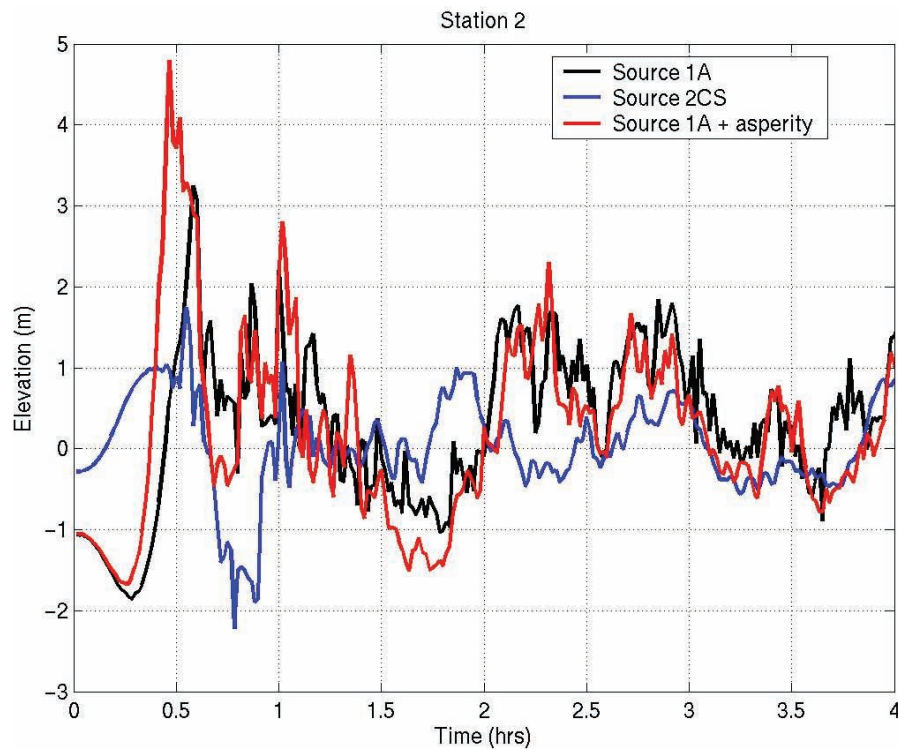


Figure 5. Current velocity changes for station 2. See Figure 1 for station location and Figure 3 caption for general explanation. Note that during the first 15–20 minutes current is surging into the estuary for the 2CS scenario but withdrawing for the other scenarios. The 2CS fault rupture is wider east-west than the other scenarios, so maximum tectonic subsidence is actually landward (east) of the observation point (see Appendix 1). The current for scenario 2CS will initially flow toward the area of maximum subsidence.

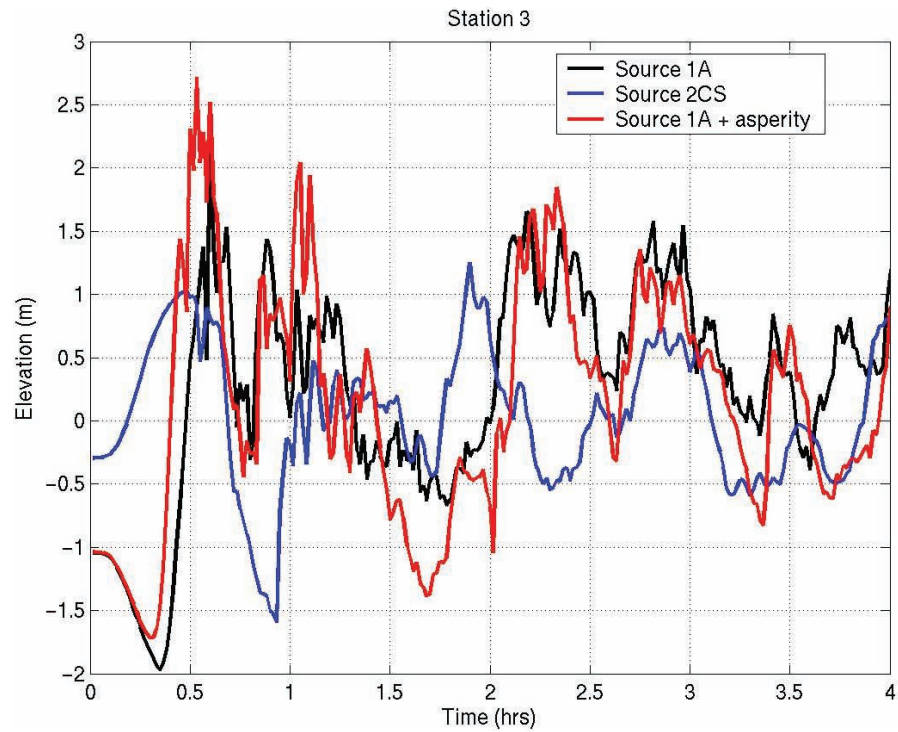


Figure 6. Station 3 time history of wave arrivals; see Figure 1 for station location and Figure 2 caption for general explanation. Note that the first wave arrives about 25–30 minutes after the earthquake.

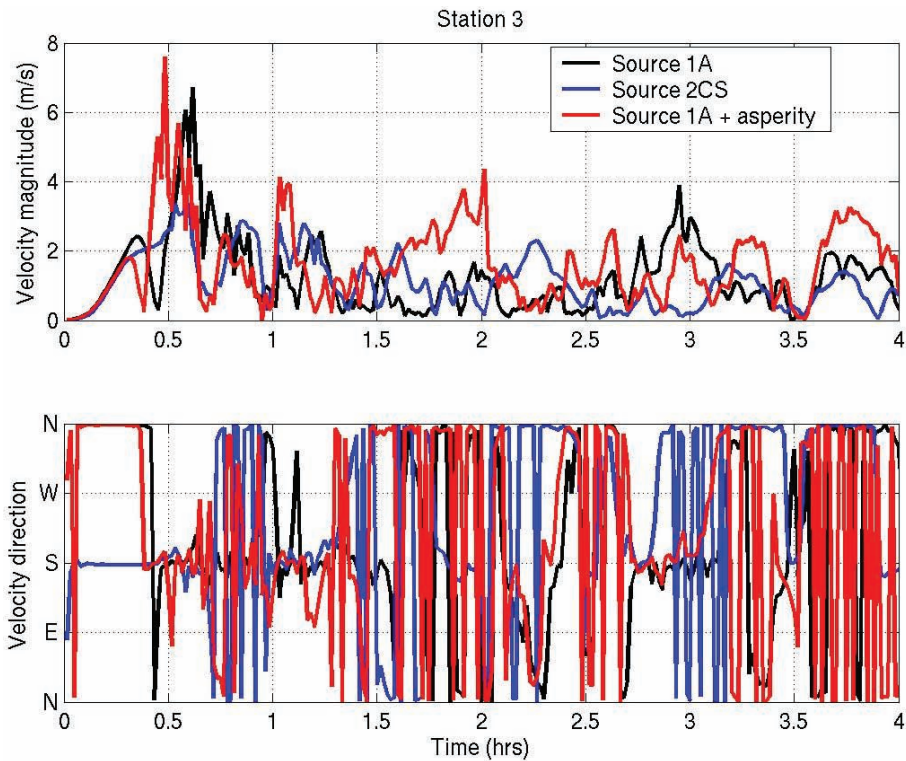


Figure 7. Current velocity changes for station 3. See Figure 1 for location and Figure 3 caption for general explanation.

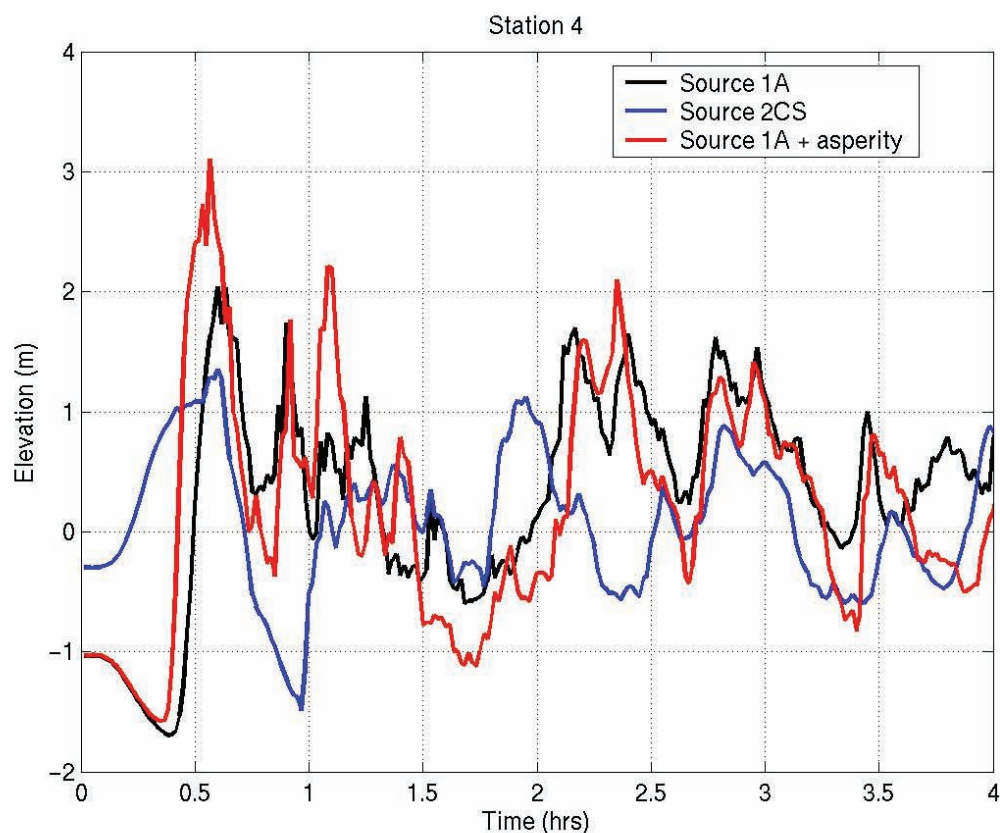


Figure 8. Station 4 time history of wave arrival; see Figure 1 for station location and Figure 2 caption for general explanation. Note that the first wave arrives ~30–35 minutes after the earthquake.

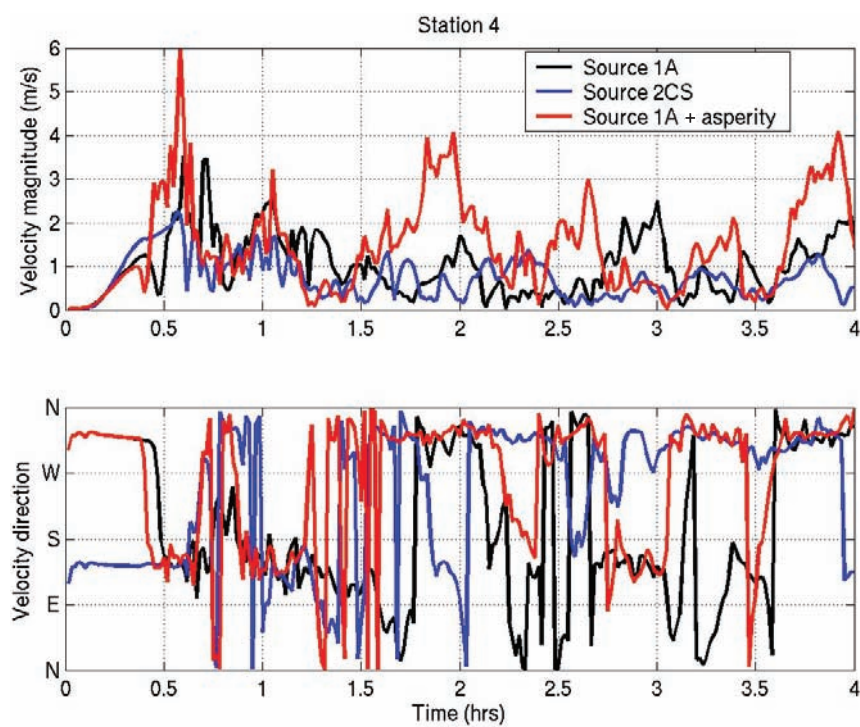


Figure 9. Current velocity changes for station 4. See Figure 1 for station location and Figure 3 caption for general explanation.

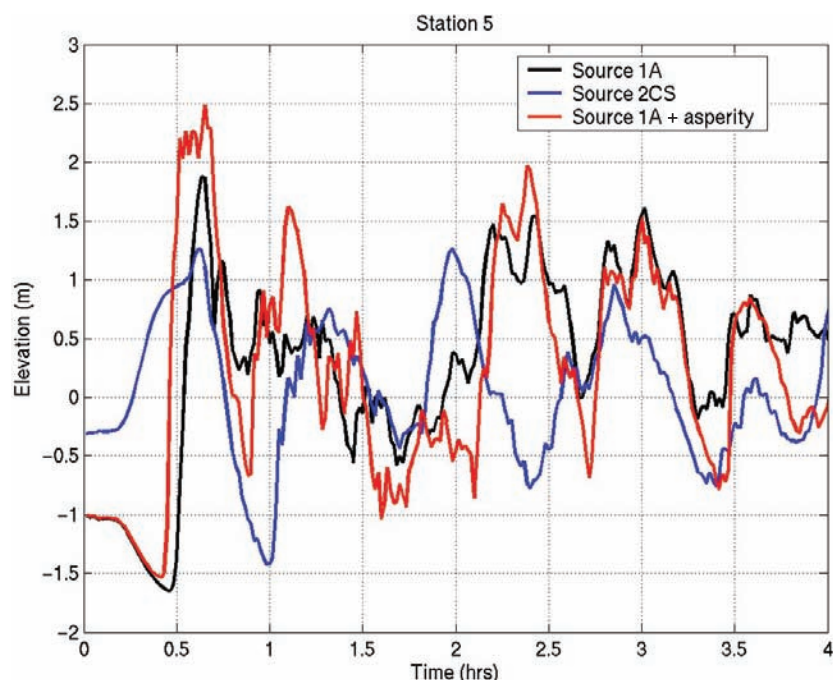


Figure 10. Station 5 (northwest Florence) time history of wave arrivals; see Figure 1 for station location and Figure 2 caption for general explanation. Note that the first wave arrives ~30–40 minutes after the earthquake.

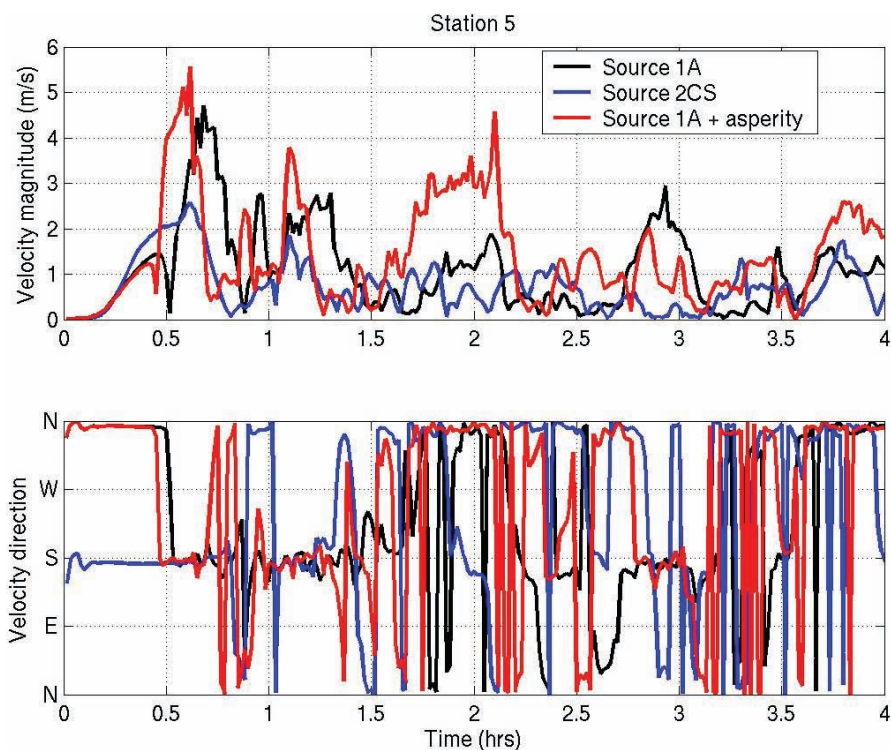


Figure 11. Current velocity changes for station 5 (northwest Florence). See Figure 1 for station location and Figure 3 caption for general explanation.

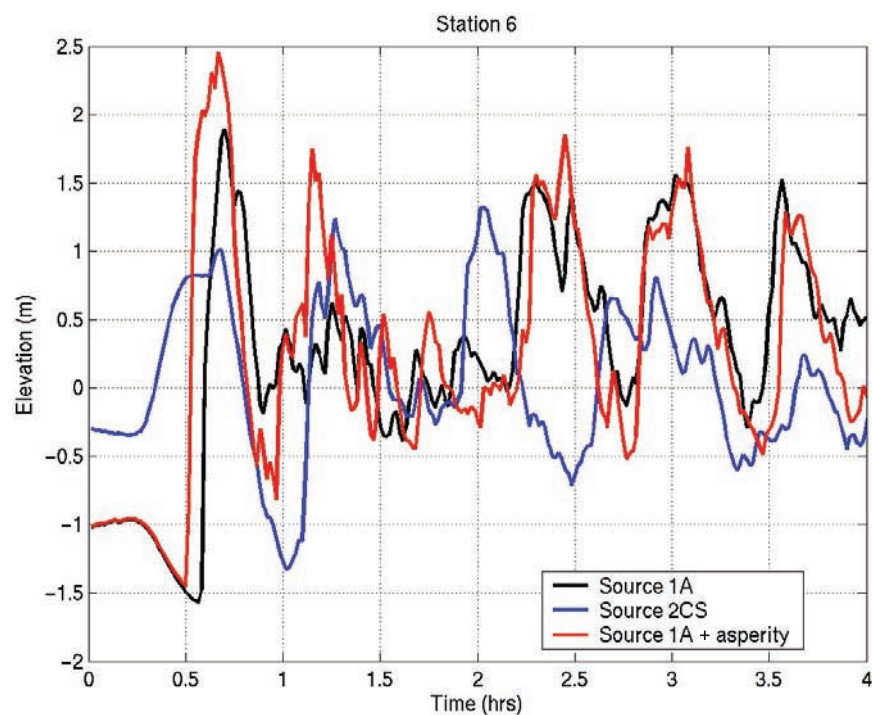


Figure 12. Station 6 (west Florence) time history of wave arrivals; see Figure 1 for station location and Figure 2 caption for general explanation. Note that the first wave does not arrive until about 35–45 minutes after the earthquake.

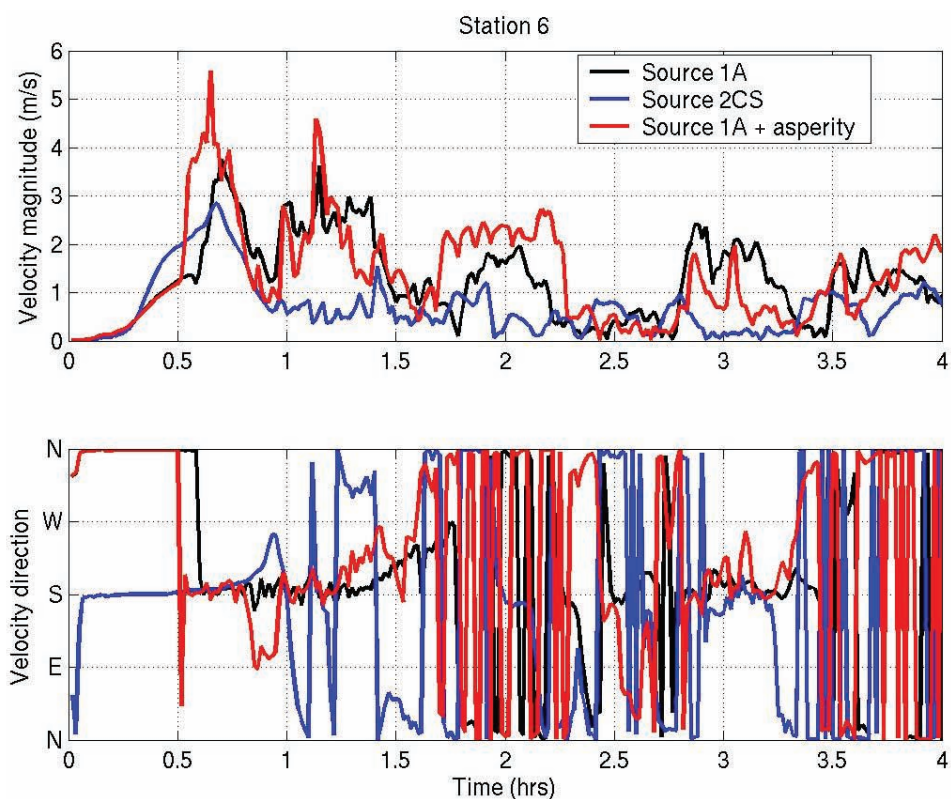


Figure 13. Current velocity changes for station 6 (west Florence). See Figure 1 for station location and Figure 3 caption for general explanation.

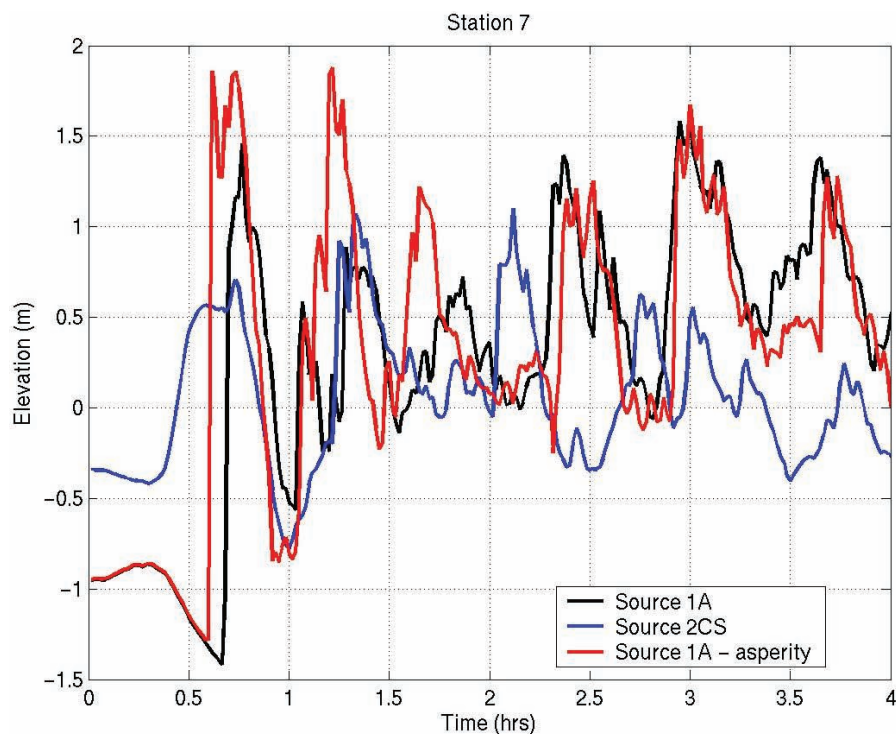


Figure 14. Station 7 (south Florence at Highway 101 bridge) time history of wave arrivals; see Figure 1 for station location and Figure 2 caption for general explanation. Note that the first wave does not arrive until about 40–45 minutes after the earthquake.

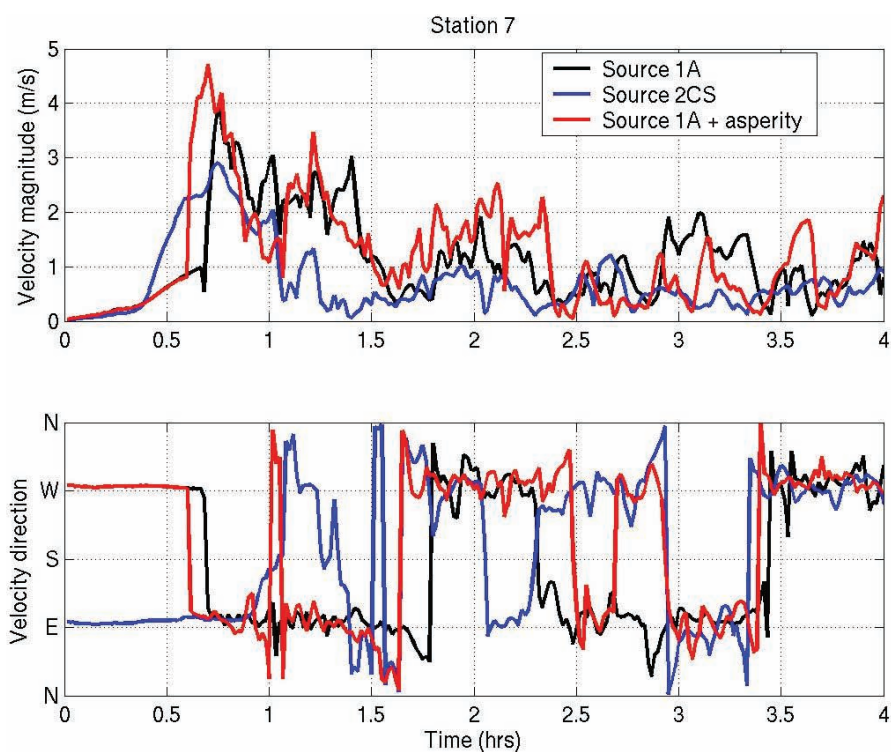


Figure 15. Current velocity changes for station 7 (south Florence at Highway 101 bridge). See Figure 1 for station location and Figure 3 caption for general explanation. There is still significant tsunami current in the estuary this far upstream.

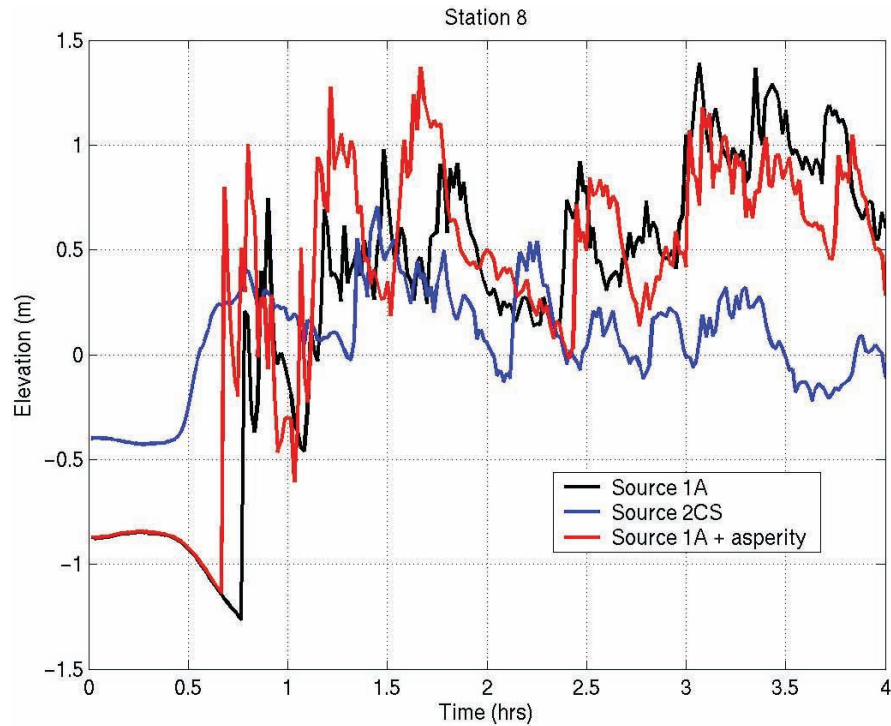


Figure 16. Station 8 (southeast Florence east of the Highway 101 bridge) time history of wave arrivals; see Figure 1 for station location and Figure 2 caption for general explanation. Note that the first wave does not arrive until about 40–50 minutes after the earthquake.

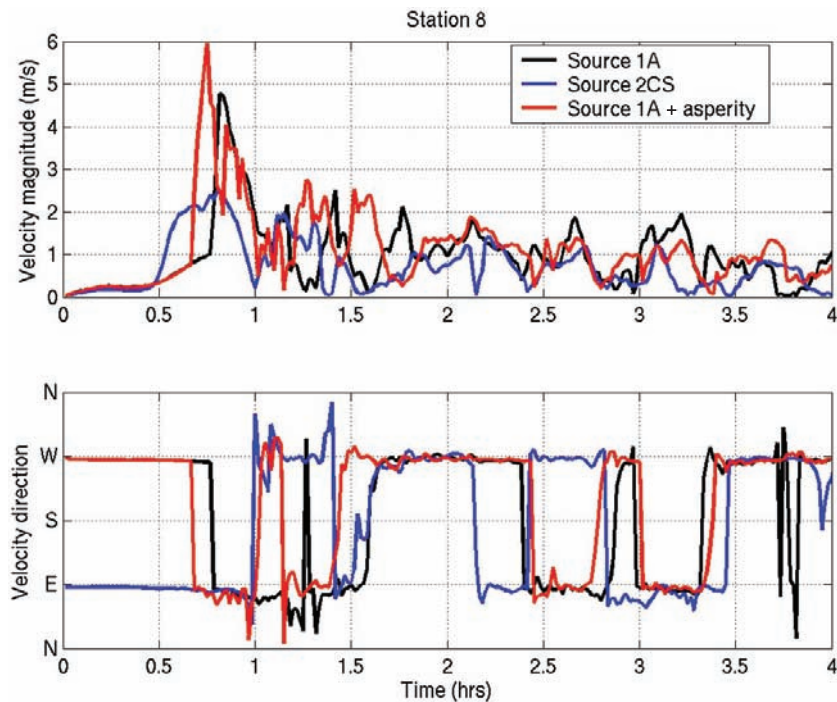


Figure 17. Current velocity changes for station 8 (southeast Florence east of the Highway 101 bridge). See Figure 1 for station location and Figure 3 for general explanation. The data illustrate that potentially damaging (8–12 knot) tsunami currents will affect the main docks and waterfront development east of the Highway 101 bridge.

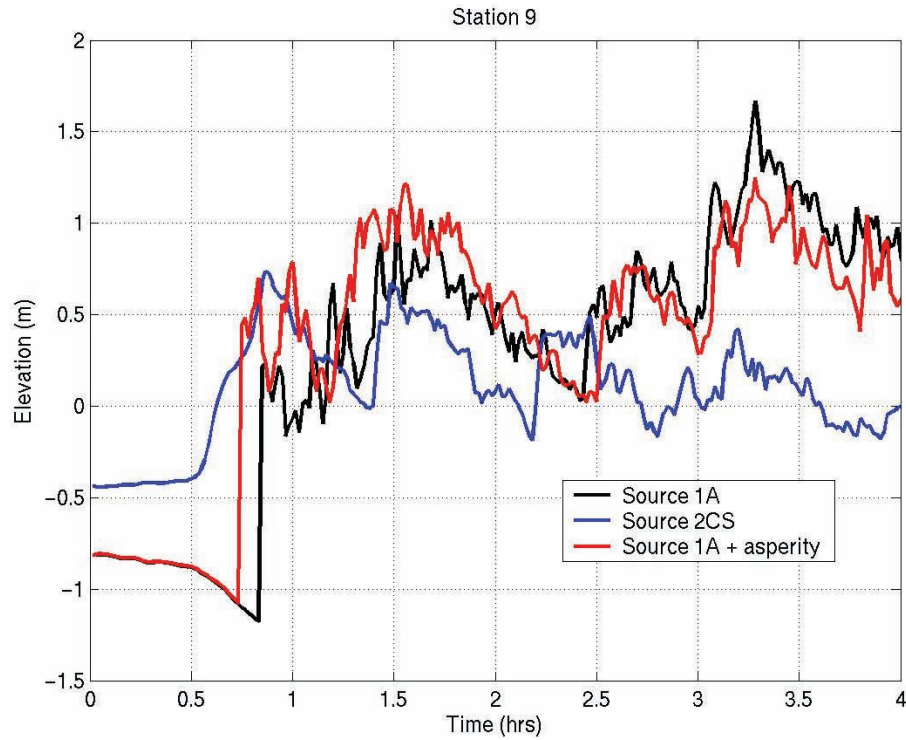


Figure 18. Station 9 (1 mile east of Florence) time history of wave arrivals; see Figure 1 for station location and Figure 2 caption for general explanation. Note that the first wave does not arrive until about 45–55 minutes after the earthquake.

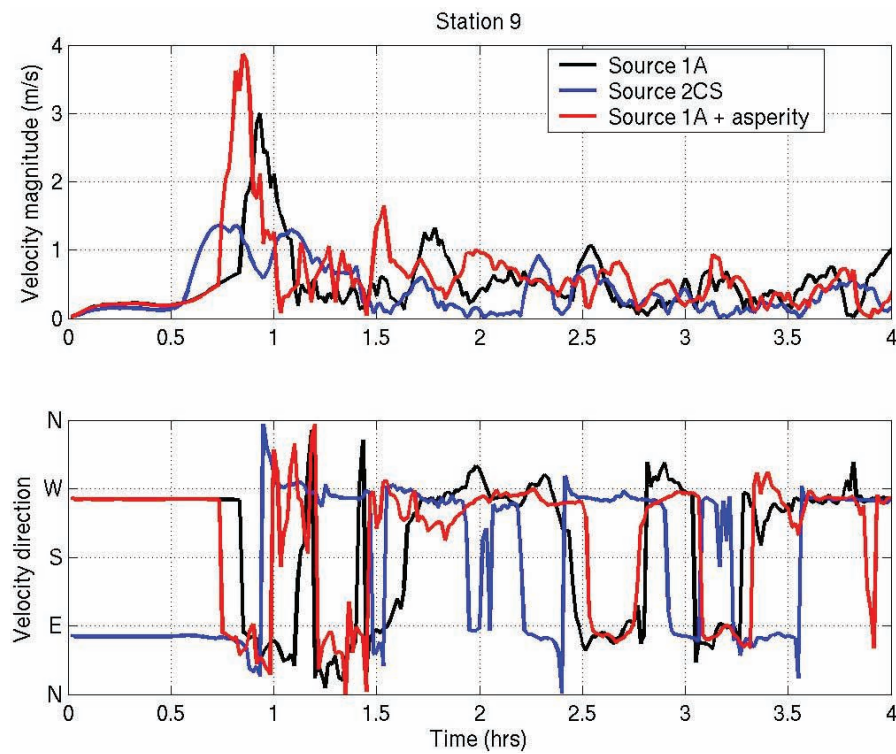


Figure 19. Current velocity changes for station 9 (1 mile east of Florence). See Figure 1 for station location and Figure 3 caption for general explanation.

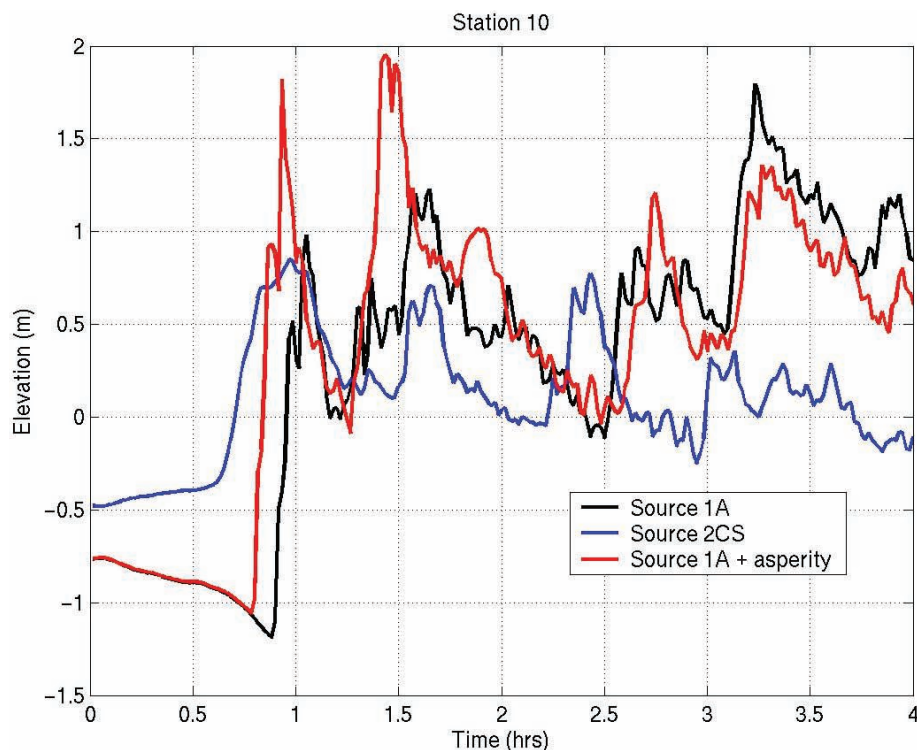


Figure 20. Station 10 (2 miles east of Florence) time history of wave arrivals; see Figure 1 for station location and Figure 2 caption for general explanation. Note that the first wave does not arrive until about 45–55 minutes after the earthquake.

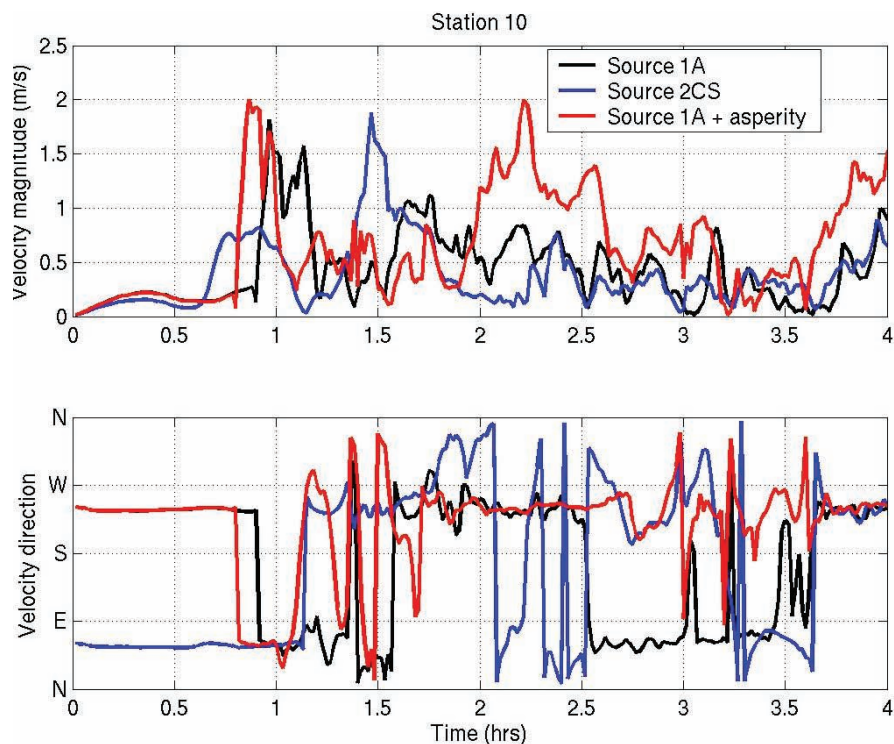


Figure 21. Current velocity changes for station 10 (2 miles east of Florence). See Figure 1 for station location and Figure 3 caption for general explanation. The relatively low velocities (3–4 knots) show that this far up the estuary much of the wave energy has dissipated.



Figure 22. Approximate area of assumed foredune erosion for large-event tsunami flooding scenario.

REFERENCES

Funding Source. Funds for the project were from National Oceanic and Atmospheric Administration (NOAA) Contract Number 50ABNR200045 under the auspices of the National Tsunami Hazard Mitigation Program (<http://www.pmel.noaa.gov/tsunami-hazard/>). Production of the map was supported by National Oceanic and Atmospheric Administration requisition number NRMAH000-6-01035.

Acknowledgements. Vasily Titov, Hal Mofjeld, and Frank Gonzalez of the NOAA Tsunami Inundation Mapping Effort (TIME) reviewed the map for technical sufficiency. The map was also reviewed by DOGAMI staff for clarity and internal consistency. Antonio Baptista of the Oregon Graduate Institute of Science and Technology, Oregon Health Sciences University, and Vasily Titov provided valuable advice and guidance for the numerical simulations. The map was field checked for accurate representation of topographic control of inundation by George Priest of DOGAMI, Ron Miller, Public Works Director, City of Florence, John Buchannon, Fire Chief, Siuslaw Valley Fire and Rescue, and Tom Kartrude, Port Manager, Port of Siuslaw.

- Allan, J. C., and Komar, P. D., 2000, Are ocean wave heights increasing in the eastern North Pacific?: EOS, American Geophysical Union, v. 81, no. 47, p. 561–567.
- Flick, R. E., Murray, J. F., and Ewing, L. C., 1999, Trends in U.S. tidal datum statistics and tide range: A data report atlas: Scripps Institution of Oceanography series No. 99-20.
- Komar, P. D., McDougall, W. G., Marra, J. J., and Ruggiero, P., 1999, The rational analysis of setback distances: Applications to the Oregon coast: Shore & Beach, v. 67, 41–49.
- Myers, E., Baptista, A. M., and Priest, G. R., 1999, Finite element modeling of potential Cascadia subduction zone tsunamis: Science of Tsunami Hazards, v. 17, p. 3–18. <http://library.lanl.gov/tsunami/ts182.pdf>
- Priest, G. R., Myers, E., Baptista, A. M., Kamphaus, R. A., Peterson, C. D., 1997, Cascadia subduction zone tsunamis: Hazard mapping at Yaquina Bay, Oregon: Oregon Department of Geology and Mineral Industries, Open-File Report O-97-34, 144 p.
- Priest, G. R., Myers, E., Baptista, A. M., Fleuck, P., Wang, K., and Peterson, C. D., 2000, Source simulation for tsunamis: lessons learned from fault rupture modeling of the Cascadia subduction zone, North America: Science of Tsunami Hazards, v. 18, no. 2, p. 77–106. <http://library.lanl.gov/tsunami/ts182.pdf>
- Priest, G. R., Baptista, A. M., Myers, E. P., III, and Kamphaus, R. A., 2001, Tsunami hazard assessment in Oregon: International Tsunami Society Proceedings, NTHMP Review Session, Paper R-3, p. 55–65. http://www.pmel.noaa.gov/ftp/AD/ryan/gonzalez/R-03_Priest.pdf

APPENDIX 1. REGIONAL TECTONIC DEFORMATION FOR THE SCENARIO EARTHQUAKES

The initial condition for the tsunami simulations is the crustal uplift and subsidence associated with the scenario earthquake. The pattern of regional crustal deformation is essentially the initial tsunami wave, as the pattern

is roughly duplicated in the sea surface above. Predicted patterns of uplift and subsidence are illustrated in Figures A1 through A3.

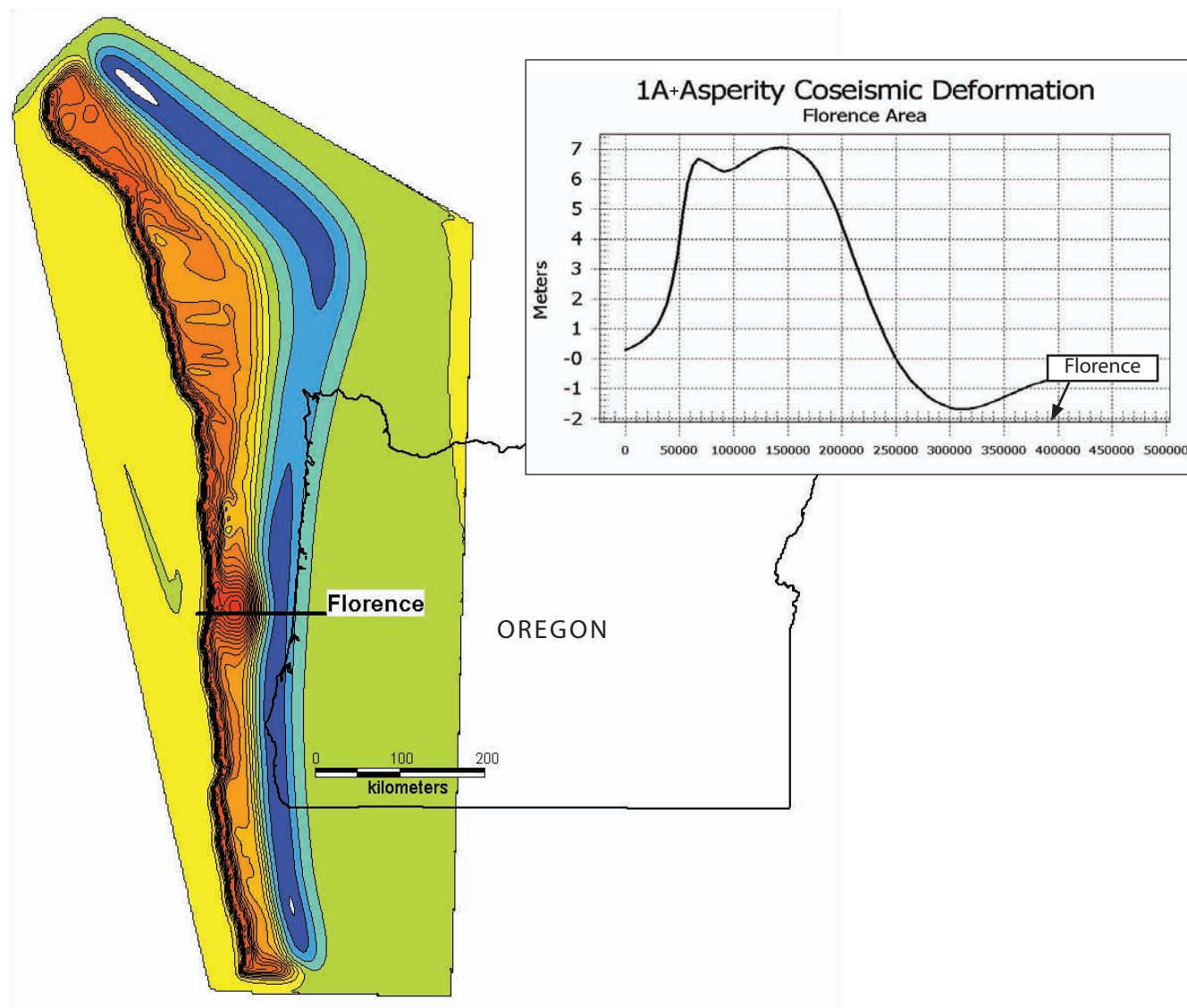


Figure A1. Ground deformation for the **large-event** scenario earthquake (scenario 1A + asperity) showing a local mound of uplift roughly twice as high as the regional ~3 m (10 ft) of uplift immediately offshore from Florence (see Figure A2 for the regional pattern without the asperity). This mound of uplift is termed an asperity and approximately corresponds to actual uplift areas observed in the magnitude 9.2 earthquake that struck Alaska in 1964. Note that up to 1 m (3 ft) of subsidence may affect parts of Florence, according to this scenario. This subsidence will likely persist for decades after the earthquake. The outline of the state of Oregon is shown for location. Note also that the mound of extra uplift is not generated by partitioning of fault slip from adjacent areas, as might be the case in an actual earthquake. If such partitioning occurred, it would lower the amount of deformation (both uplift and subsidence) surrounding the area of concentrated fault slip.

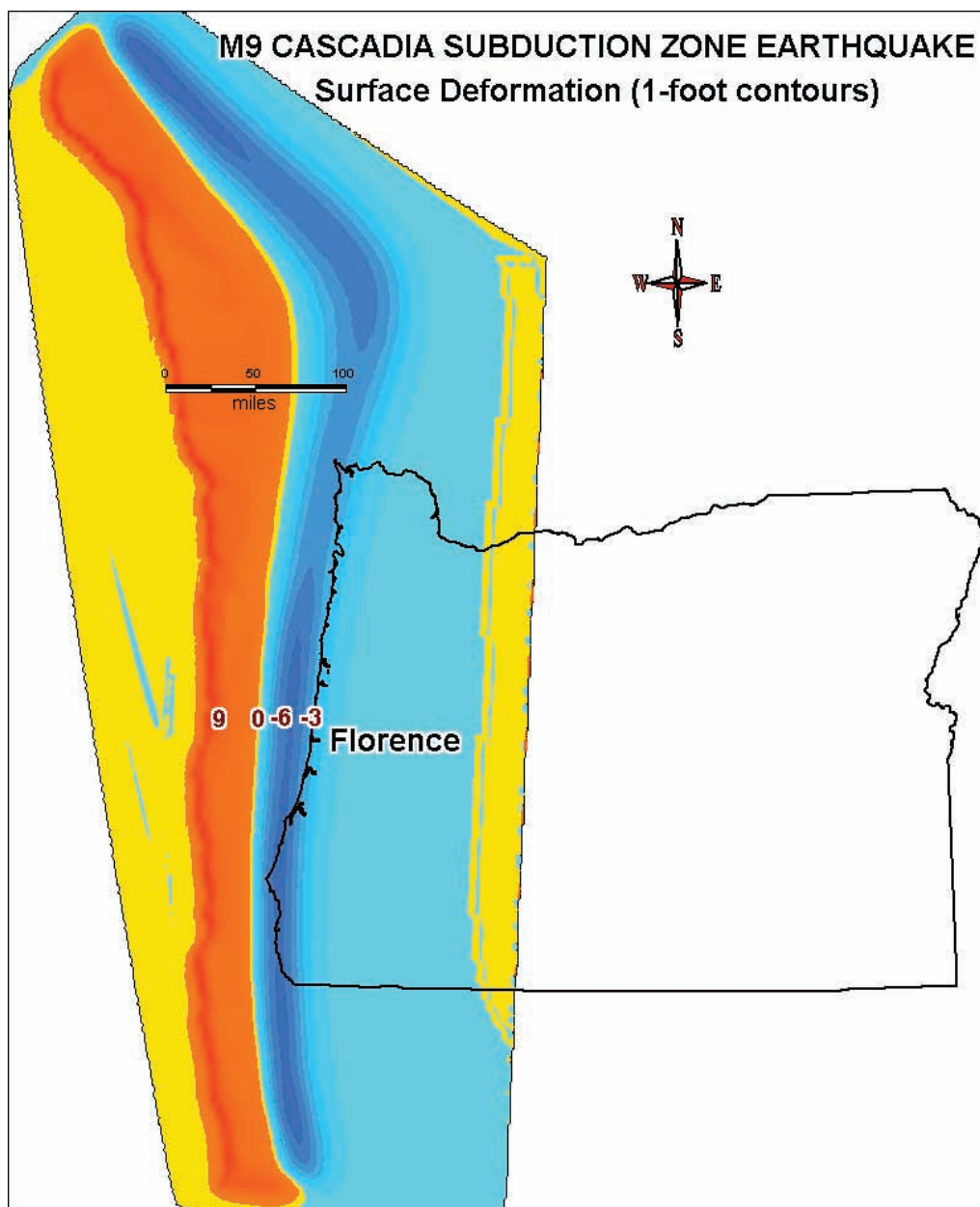


Figure A2. Crustal deformation for the average-event inundation scenario (scenario 1A) is essentially the same as the large-event scenario (~10 m [3 ft] of subsidence in Florence) but without the asperity offshore. Brown numbers are in feet, negative numbers indicate subsidence; positive numbers indicate uplift.

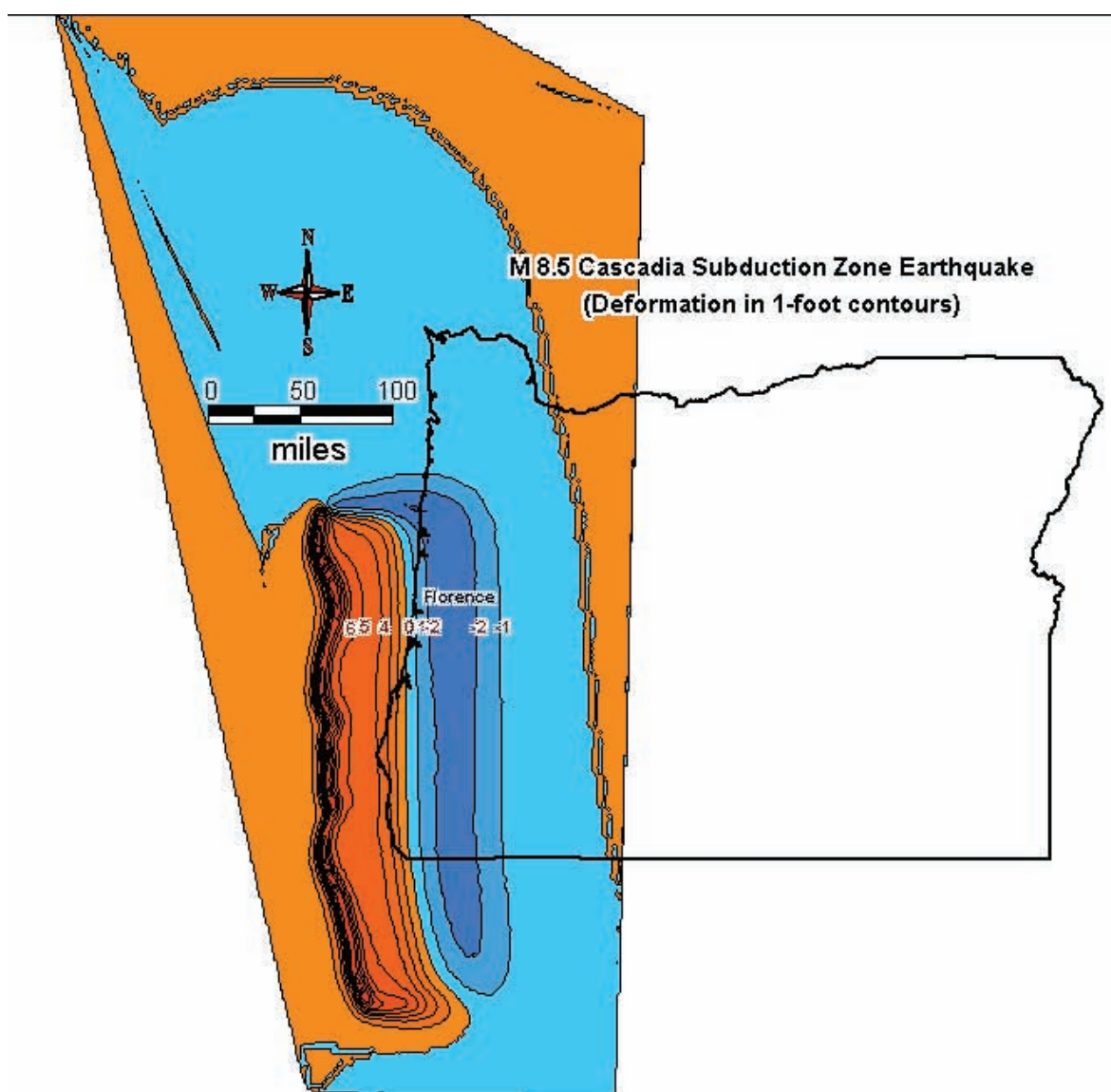


Figure A3. Small-event earthquake deformation (scenario 2Cs). Blue regions are coseismic subsidence; orange regions are coseismic uplift; brown numbers are in feet, negative numbers indicate subsidence; positive numbers indicate uplift. This scenario assumes that only the southern portion of the subduction zone ruptures and that total fault displacement will be about half that of the average-event scenario. This scenario also assumes a somewhat wider rupture, which is supported by some geological studies (see Priest and others, 1997, for discussion). Wider ruptures, all other things being equal, create lower elevation tsunamis than narrow ruptures in this geological setting, because the initial wave amplitude (vertical distance between wave crest and wave trough) is smaller. This is the case, because the subsidence is on dry land in the wider rupture and does not affect amplitude at sea. Note that only ~0.5 m (1 ft) of subsidence occurs at Florence for scenario 2Cs.

APPENDIX 2. ESTIMATED WATER DEPTH FOR THE LARGE-EVENT TSUNAMI FLOODING SCENARIO, 1A + ASPERITY

This appendix shows computer-contoured water depths in 2-ft contours for the large-event tsunami flooding scenario, 1A + asperity. Only populated areas are illustrated. The inundation boundary is shown as a bold red line and can be considered the 0-ft depth line. All inundation boundaries in this publication are inferred from the computer simulation and available topographic data. The topographic data are in all cases much more detailed than the topography that could be inferred from the computational bathymetric grid used by the computer simulation to derive water depths. The computer is thus unable to “see” topographic details during the simulation, but we use these details when drawing the inundation boundary at elevations that are reasonable interpretations of the numerical simulation.

Water depth reflects the maximum tsunami water elevation reached during the computer simulation, the water depth increase from coseismic subsidence during the earthquake, and tide at 1.28 m (~4 ft) above geodetic (NAVD29) mean sea level (i.e., tide at mean higher high water). In most cases the maximum water depth was reached when the first tsunami surge struck.

The spacing between numerical calculation nodes (output data from the numerical simulation) is on the

order of 15 m (50 ft) for populated areas of the Siuslaw Estuary (Figure A4b). Spacing decreases smoothly away from the estuary, leading to less and less ability of the contouring program to discern rapid changes in depth caused by local topographic features (see Figures A13 through A16). In this regard, the northern part of Heceta Beach has a coarse grid with relatively inaccurate depth contours (Figure A16). Even where the spacing is 15 m (50 ft), the grid is still too coarse to accurately resolve the rapid depth changes at near vertical estuary banks, so contours are only approximate in areas of rapid slope change. In many cases depth contours with relatively large values end abruptly at the inundation boundary. This is an artifact of the contouring method whereby the contouring program smoothed the contours across areas with no inundation (zero values or no data). These anomalous contours were deleted outside of the inundation polygon using GIS editing software, leading to many contours ending at high angles against the boundary; nevertheless, the contours give a general idea of how water depth varies, being most accurate in areas of gentle slopes and wide spread inundation where many numerical nodes are available to simulate the flooding area.

Figure A4. (facing page) (a) Tsunami water depth contours (yellow lines) in feet (red labels) for the 1A + asperity scenario with mapped inundation (red line). Mapped inundation is inferred to extend somewhat beyond the last wet numerical grid point in the computer simulation. Mapped inundation also takes into account small features such as drainages and ravines that could not be accurately simulated (“seen” by the computer model) at the grid spacing. Area shown is the southeast side of downtown Florence. Base map is a U.S. Geological Survey digital orthophoto quadrangle compiled from aerial photography flown about 1994. Street names are taken from digital data on Lane County streets compiled by the Oregon Department of Transportation (<http://www.oregon.gov/ODOT/TD/TDATA/gis/dgnfiles.shtml>).

(b) Illustration of the 15-m (50-ft) numerical grid used to derive depth contours in populated portions of the Siuslaw Estuary. Area is the same as in Figure A4a.

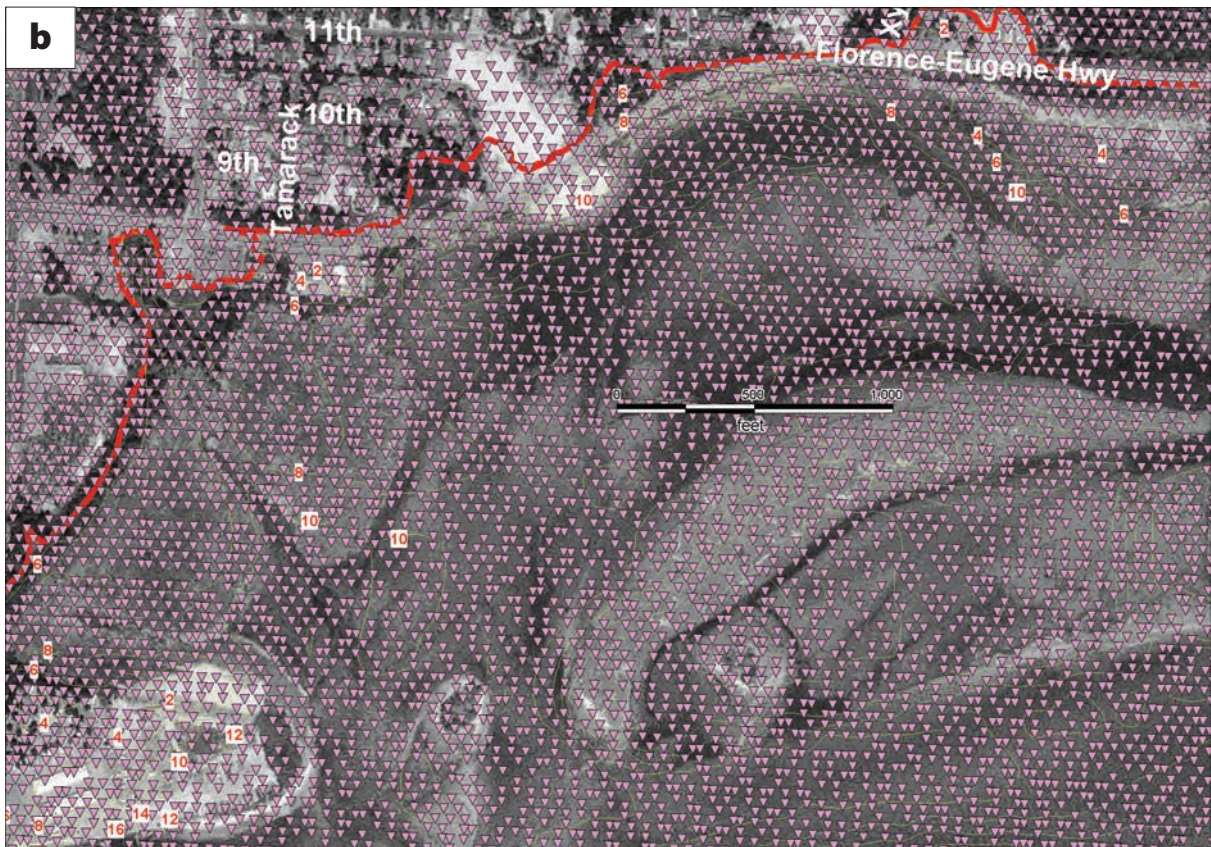




Figure A5. Downtown Florence (Old Town area). See Figure A4 caption for explanation.

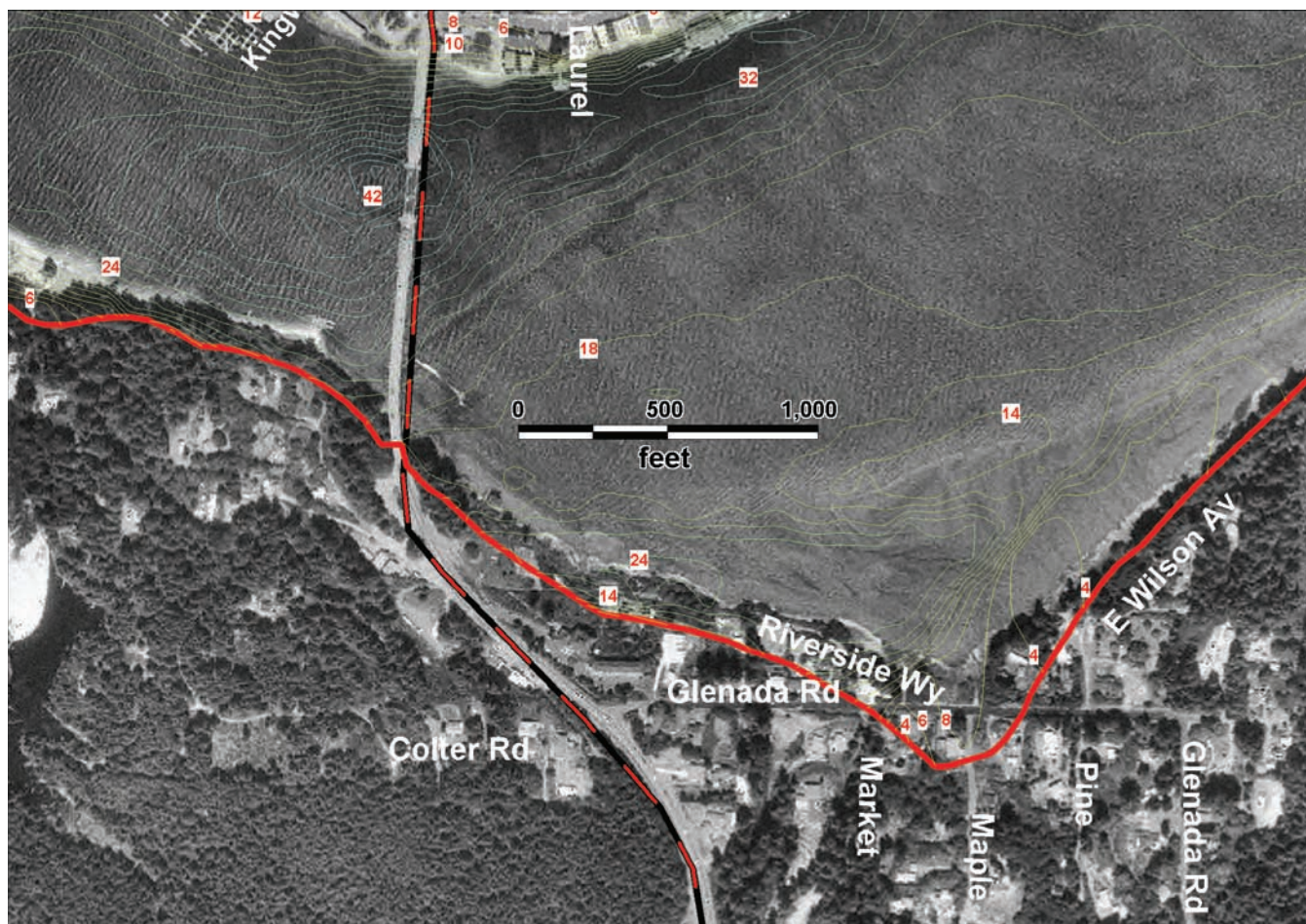


Figure A6. Florence area on the south side of the Highway 101 bridge. See Figure A4 caption for explanation.



Figure A7. Florence and adjacent sand spit, immediately northwest of the Old Town area. See Figure A4 caption for explanation.

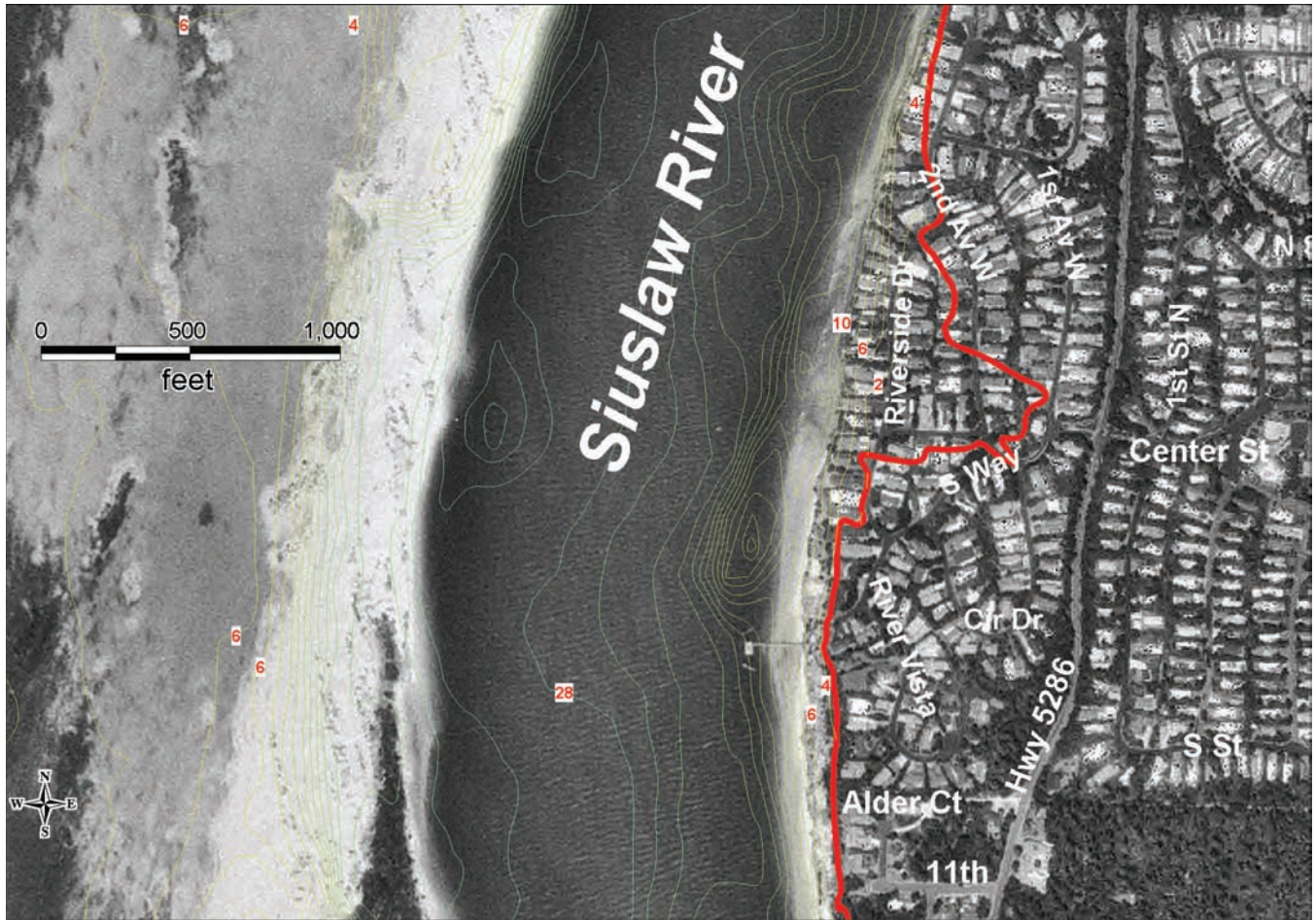


Figure A8. Northwest Florence between 11th and 1st Avenue West at Riverside Drive. See Figure A4 caption for explanation.

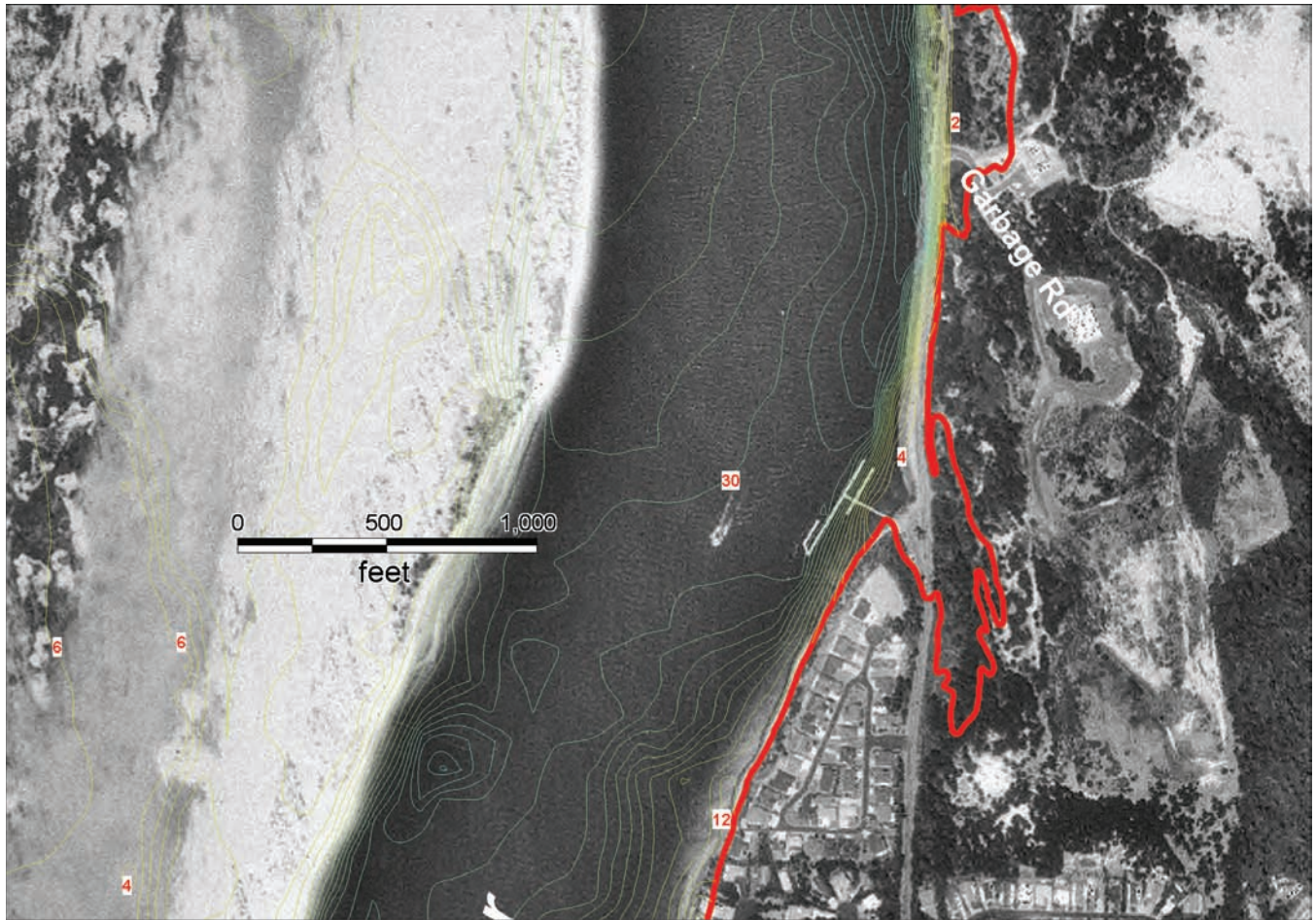


Figure A9. Northwest Florence in the vicinity of the local landfill. See Figure A4 caption for explanation.

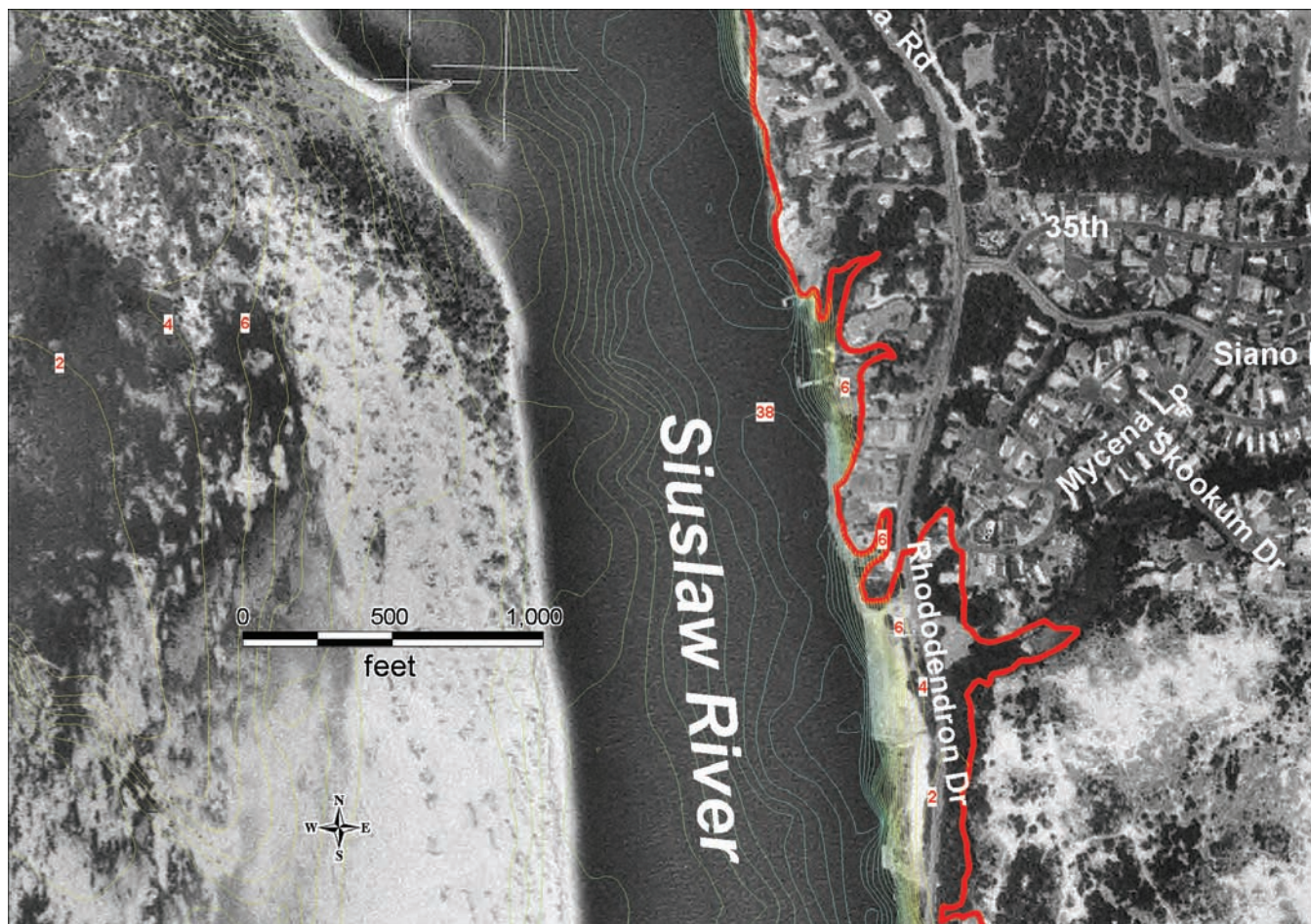


Figure A10. Northwest Florence in the vicinity of 35th and Rhododendron Drive. See Figure A4 caption for explanation.



Figure A11. Northwest Florence in the vicinity of the Coast Guard station. See Figure A4 caption for explanation.

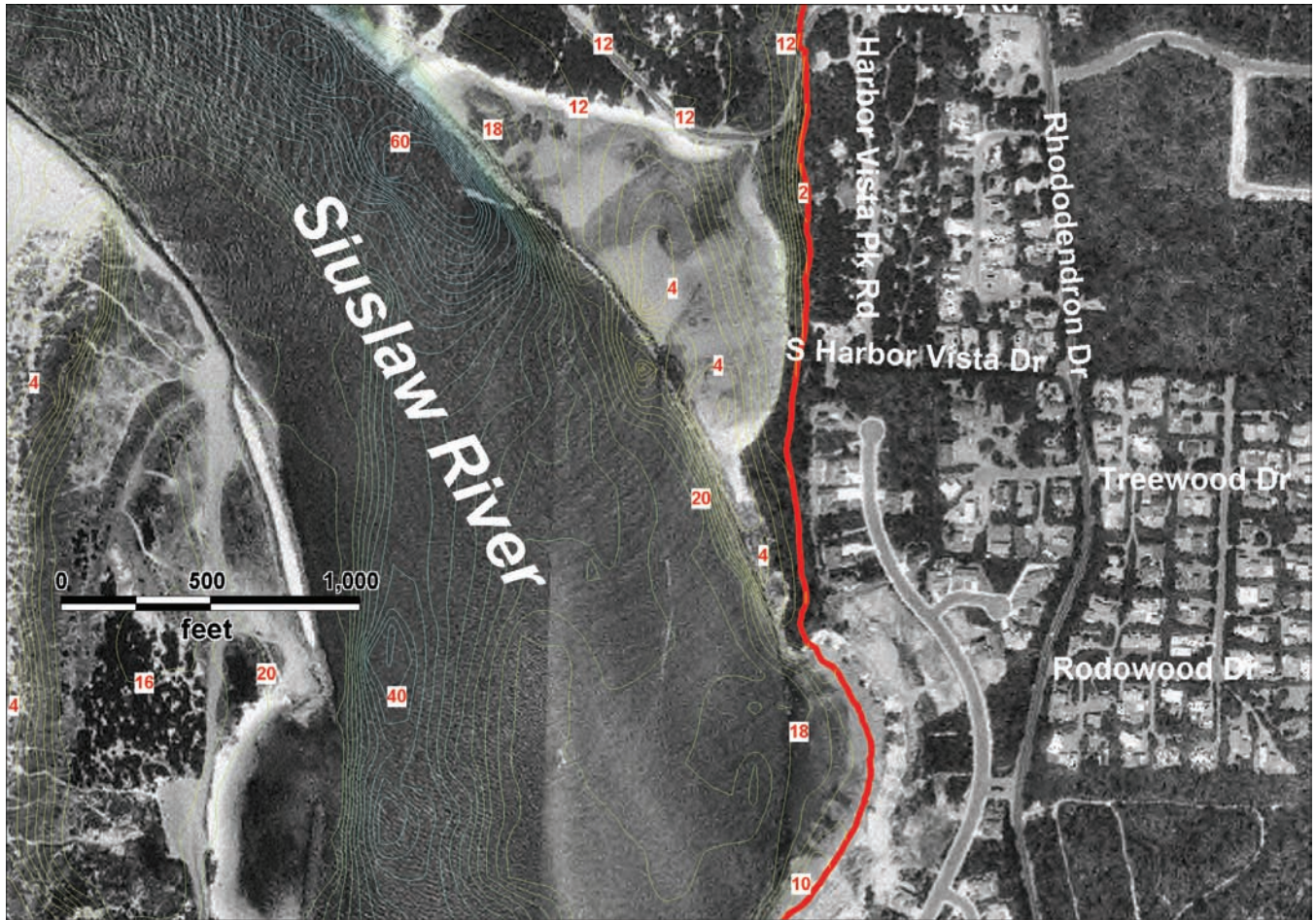


Figure A12. Mouth of the Siuslaw River in the vicinity of Harbor Vista Park Road. See Figure A4 caption for explanation.



Figure A13. Heceta Beach immediately north of the of the Siuslaw River in the vicinity of North Jetty Road to Woodlands Drive. Purple triangles are the numerical grid in this area; note that spacing increases away from the estuary. See Figure A4 caption for explanation of depth contours and labels.

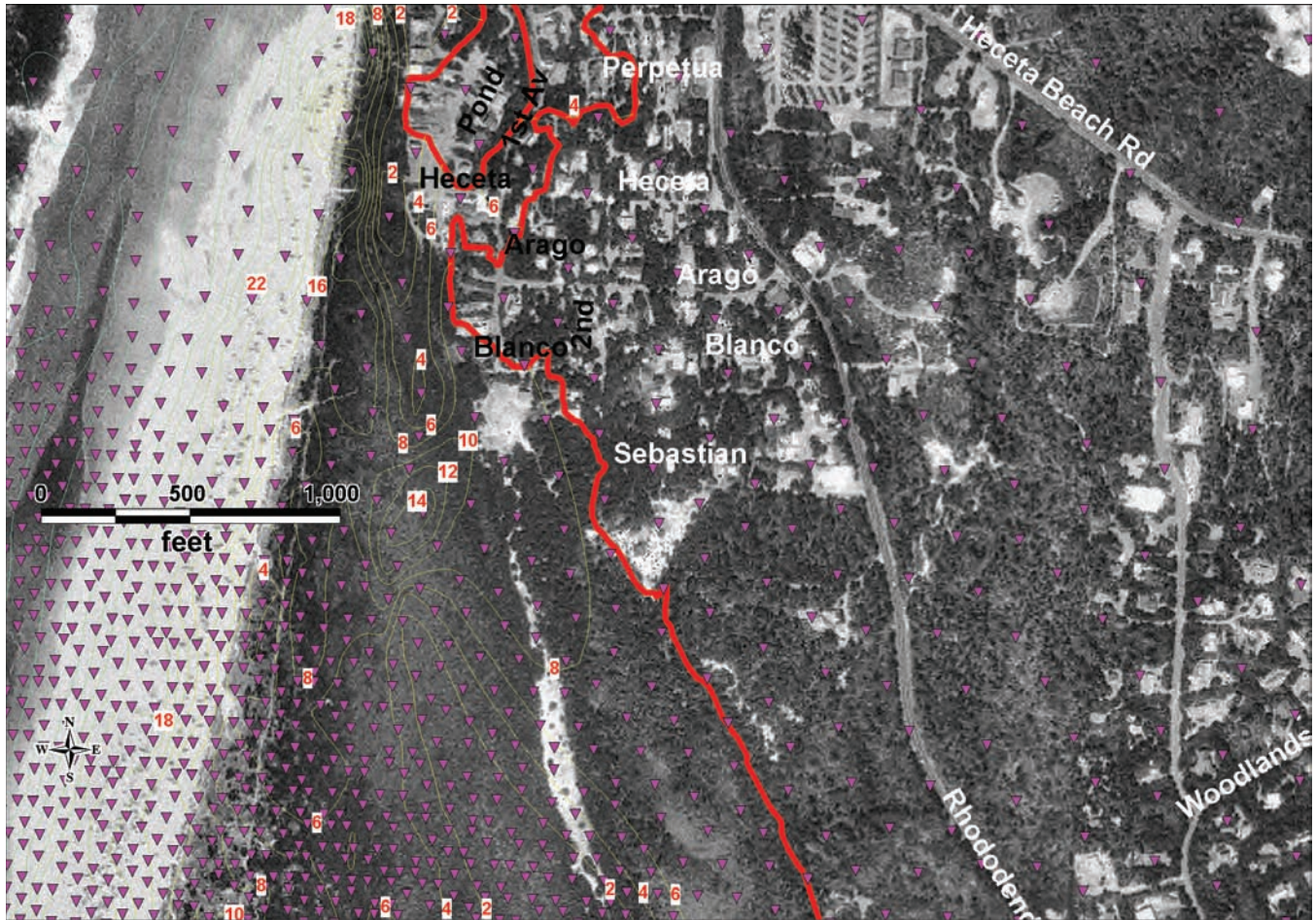


Figure A14. South Heceta Beach in the vicinity of Perpetua and Sebastian Roads. Note how the numerical grid spacing (purple triangles) continues to increase away from the mouth of the estuary to the south. See Figure A4 caption for explanation of depth contours and labels.

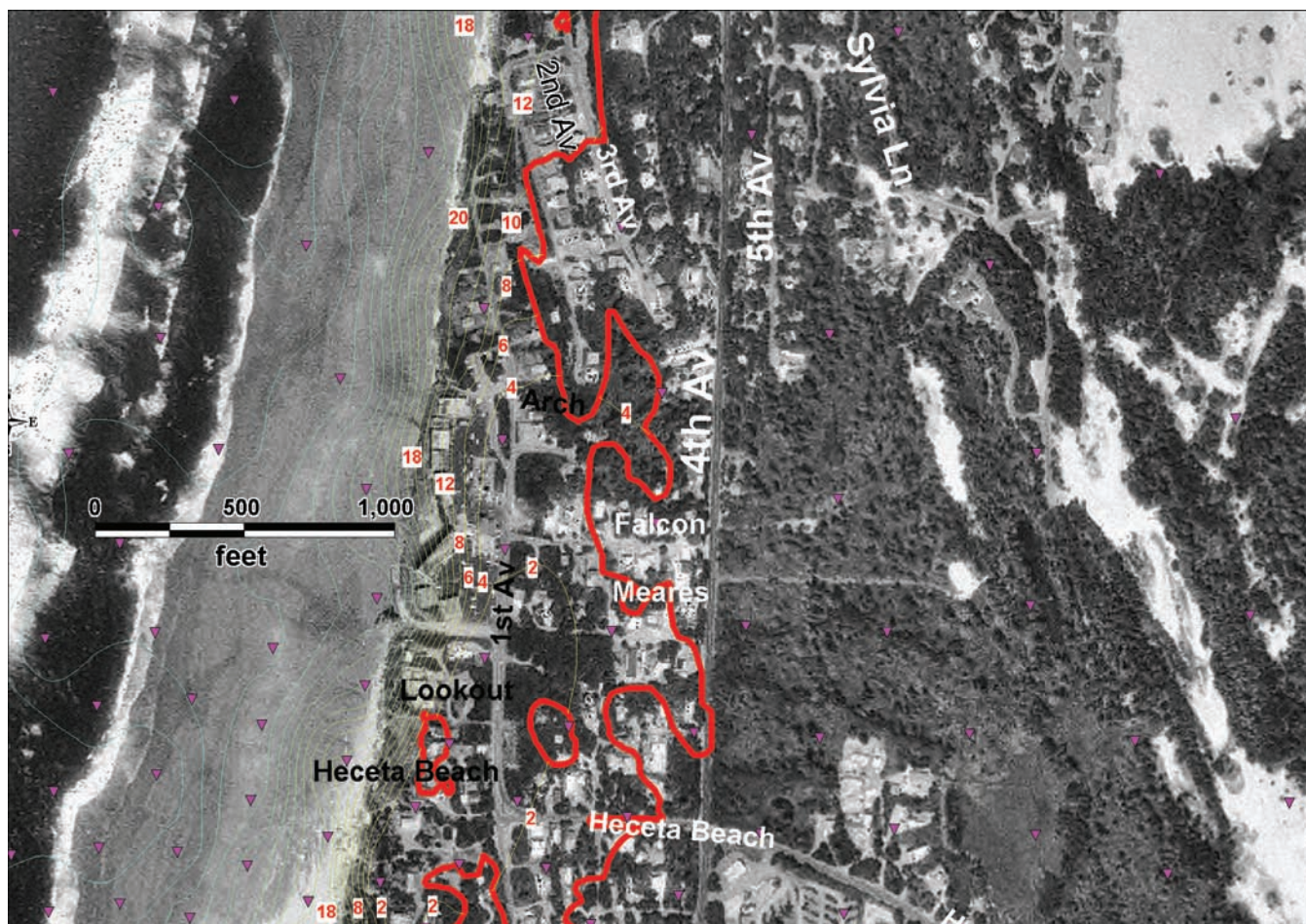


Figure A15. Central Heceta Beach from Heceta Beach Road to 2nd Avenue. Note how the numerical grid spacing (purple triangles) continues to increase away from the mouth of the estuary to the south. Depth contours are of limited accuracy in this area because of the wide spacing. See Figure A4 caption for explanation of depth contours and labels.

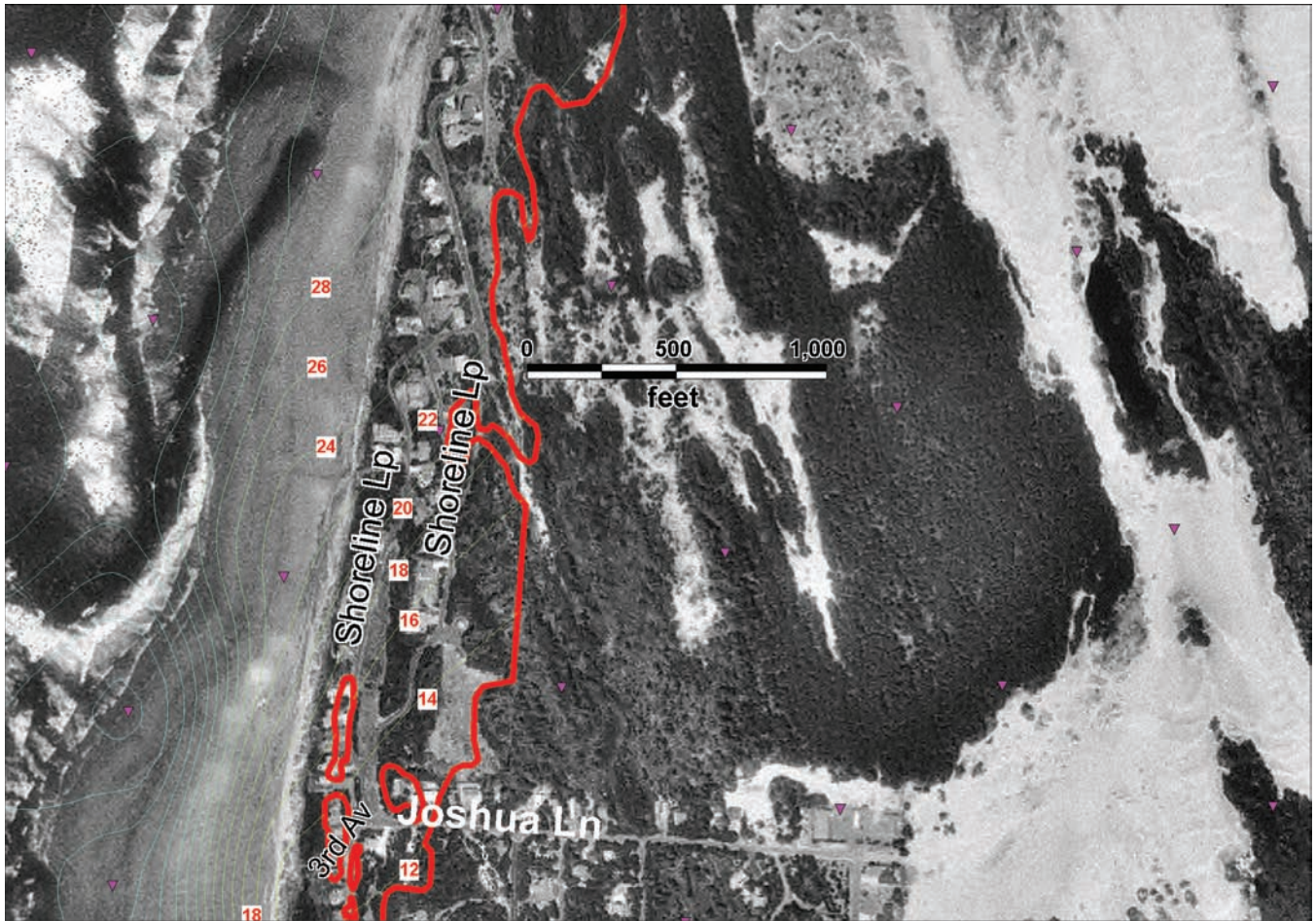


Figure A16. North Heceta Beach from Joshua Lane to Shoreline Loop. Depth contours in the northern part of this area have poor accuracy owing to wide spacing of numerical grid points (purple triangles) and smoothing of the depth contours by the computer program. See Figure A4 caption for explanation of depth contours and labels.

APPENDIX 3. EXPLANATION OF ENERGY COMPENSATION²

One of the tests of the accuracy of the Cascadia event tsunami simulations for the town of Florence was to see if mass and energy were conserved inside the computational domain. Mass conservation was achieved to within less than 1% for the entire length of the simulation. Energy conservation was a completely different matter. The numerical model is a two-dimensional shallow water wave model and accounts for bottom drag but not wave breaking. The total energy in the model is thus given by

$$E = E_{PE} + E_{KE} - E_{FE} - E_{flux} \quad (A3:1)$$

where E , E_{PE} , E_{KE} , and E_{FE} represent the total energy, the potential energy, the kinetic energy, and frictional energy loss over the entire domain, respectively. E_{flux} represents the total (potential and kinetic) energy flux across the open boundaries.

Potential and kinetic energy terms for depth-averaged processes are given by

$$E_{PE} = \frac{1}{2} \rho g \iint_{\Omega} \eta^2 d\Omega \quad (A3:2a)$$

$$E_{KE} = \frac{1}{2} \rho \iint_{\Omega} (\eta + h)(u^2 + v^2) d\Omega \quad (A3:2b)$$

where η , u , v , ρ , g , d , and t represent the surface elevation, east-west velocity, north-south velocity, water density, acceleration due to gravity, distance, and time, respectively, and Ω represents the computational domain of the model. Because the model uses a quadratic bottom friction formulation, energy dissipation due to bottom friction is defined by

$$E_{FE} = \int_t \rho \iint_{\Omega} C_d (u^2 + v^2)^{3/2} d\Omega dt \quad (A3:3)$$

C_d in equation A3:3 is the nondimensional bottom drag coefficient that varies with depth and is based on

the Manning formulation; its maximum value is on the order of 0.0006.

For the model to conserve energy, E in equation A3:1 should remain unchanged. In the simulations, the distance between the source and the open boundary was much greater than the distance between land and the source. Thus, during the first few waves coming to land, there is minimal energy flux through the open boundaries. This precludes the need to compute E_{flux} in equation A3:1.

To evaluate the ability of the numerical model to conserve energy and the accuracy of the energy tracking algorithm a Gaussian (bell-shaped) hump was propagated in a straight channel with constant depth. The model was able to conserve energy to within 1% until the wave reached the open boundary. Thus, for simple domains, the numerical model conserves energy very well. In the Florence simulations, however, we found that the energy consistently drops over the first two hours of the simulation period (Figure A17). This drop in energy arises from the fact that the potential energy decreases much faster than the corresponding increase in kinetic energy. The mismatch cannot be explained by either the frictional energy losses (which are an order of magnitude smaller for this case) or energy fluxes across the open boundaries (as the domain in this simulation is large enough that none of the waves made it to the open boundary during this time period). Energy conservation did not improve by increasing the grid resolution (either offshore or near the coast). It remains to be seen whether this is a problem associated with this particular model or whether other models based on shallow water equations face similar limitations.

In the mean time, to develop realistic estimates for inundation, we increased the initial uplift to increase the total energy into the system to compensate for energy loss (at least in the first two hours of the simulation when the major inundation occurs). Uplift was added over the entire domain but only in the parts where there was uplift (not in the subsidence area). It was also weighted by uplift calculated by the fault dislocation model prior to the energy correction. This allowed most of the addition to be in the regions with the greatest uplift. Thus, in regions with very little (but positive) uplift there was very little energy added, while in regions with strong uplift the energy added was much larger.

2. Dr. Arun Chawla, formerly of Oregon Graduate Institute of Science and Technology, Oregon Health Sciences University wrote this section and did the computer simulations for all of the hazard scenarios. At this writing Dr. Chawla is with the National Oceanic and Atmospheric Administration (NOAA), Pacific Marine Environmental Laboratory, Seattle, Washington.

Figure A18 shows the energy comparisons before and after adding the extra energy. The required increase in the uplift (for the 1A + asperity case) necessary for providing this additional energy is demonstrated in Figures A19 through A21, which show the deformation both before and after the additional energy is added to the system. Figure A22 illustrates the effect on inundation of adding the lost energy.

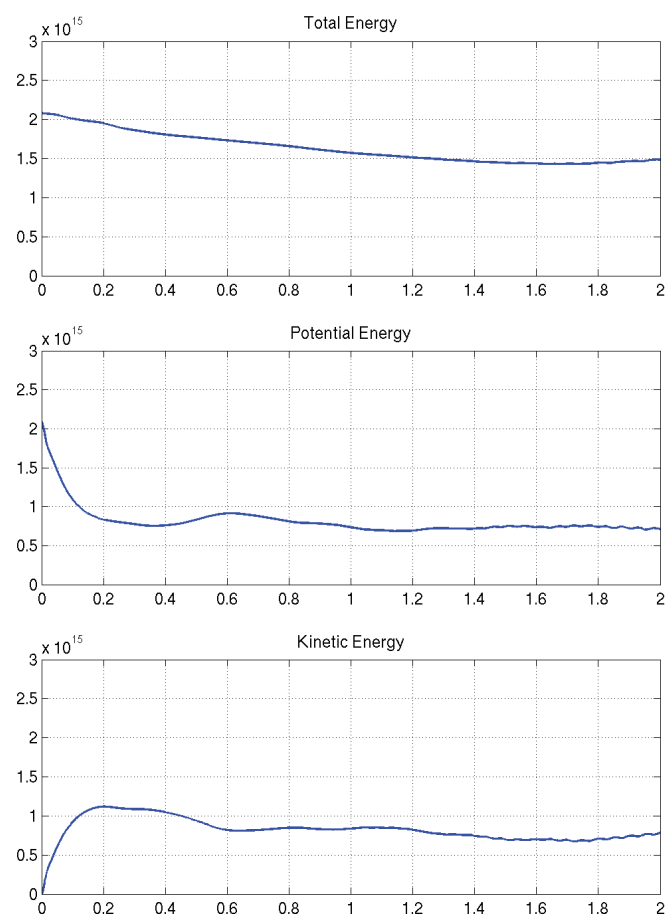


Figure A17. Energy versus hours of simulation (wave travel time) for the 1A + asperity simulation. The other two simulations (2Cs and 1A) have similar energy losses. Horizontal axis shows hours of simulated tsunami travel.

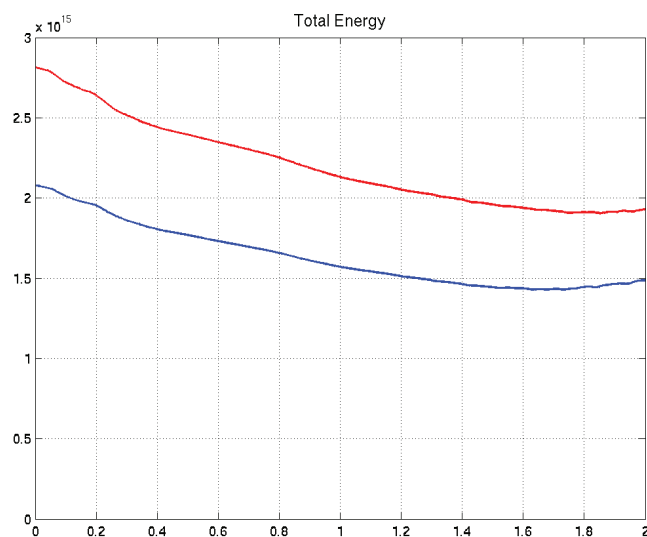


Figure A18. Comparison of total energy losses before (blue line) and after (red line) adding compensating energy. Horizontal axis shows hours of simulated tsunami travel.

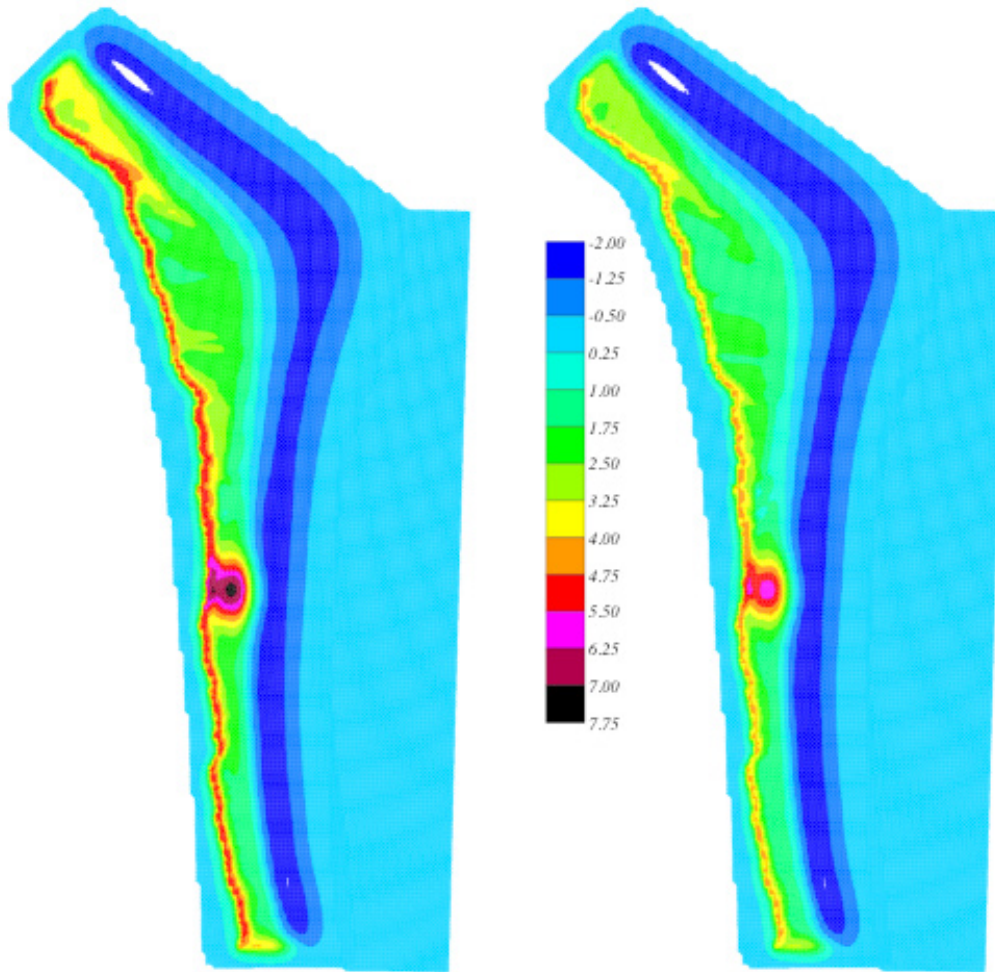


Figure A19. Uplift in meters for the 1A + asperity simulation before (right) and after (left) initial wave elevation is added to compensate for energy losses. Similar wave height was added to the 2Cs and 1A simulations.

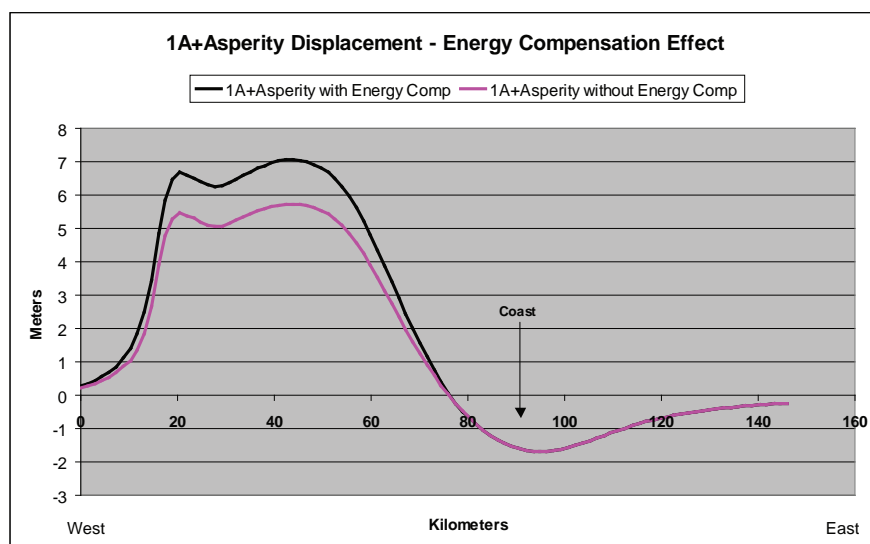


Figure A20. Comparison in cross section of initial displacement for 1A + asperity scenario before and after elevation is added to compensate for energy losses. Comp is compensation. Scenarios 2Cs and 1A had displacement added proportionally the same way in offshore areas. See Figure A21 for location.

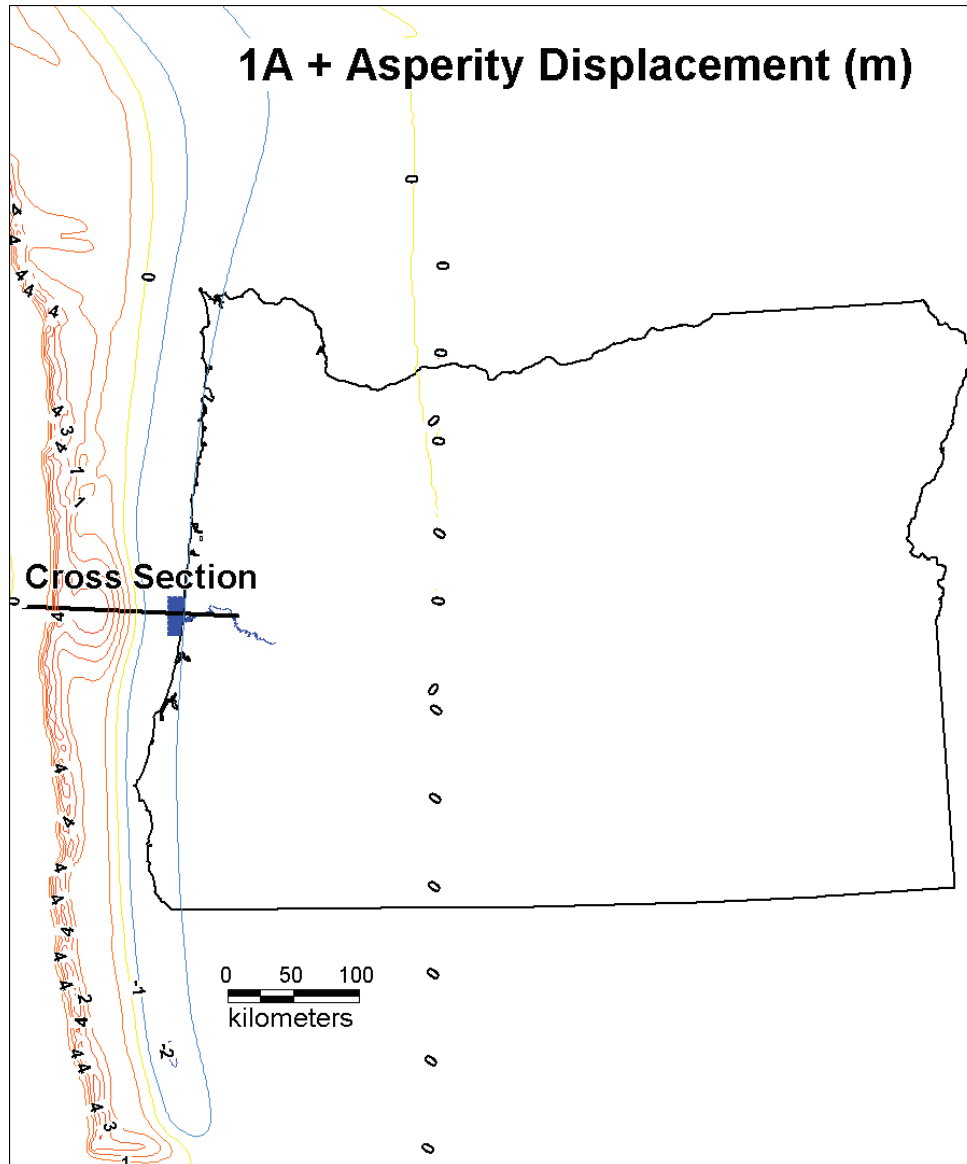


Figure A21. Location of cross section in Figure A20. Blue line is the Siuslaw Estuary; Contours are initial water surface displacement in meters without addition of height to compensate for energy losses.

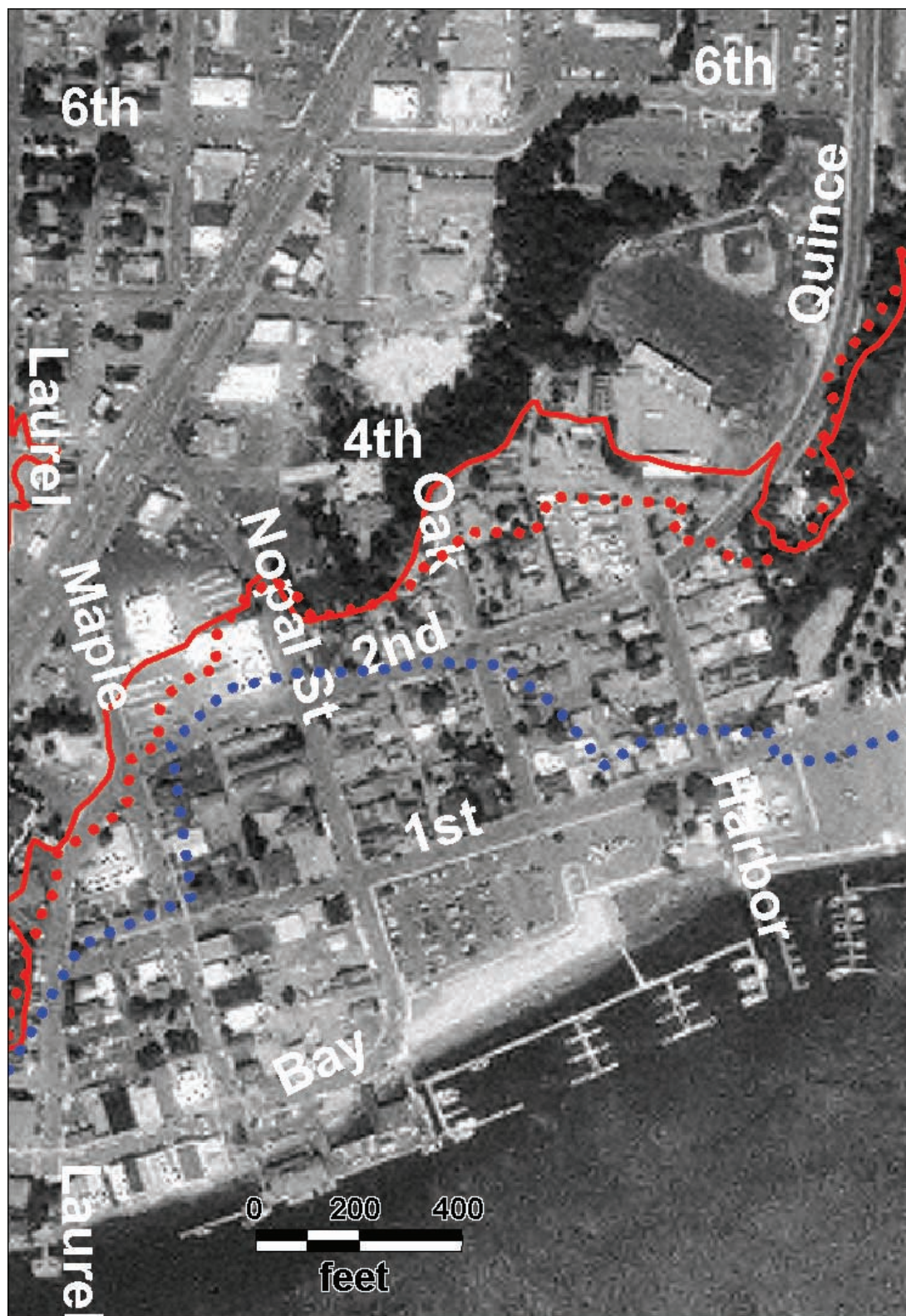


Figure A22. Large flooding event (1A + asperity) inundation in downtown Florence with energy compensation (red dots) and without energy compensation (blue dots). Dotted lines drawn to connect first dry numerical node in each case. Red solid line is final mapped inundation boundary inferred from the simulation (red dots) and local topographic contours at elevation intervals of 2 ft.

APPENDIX 4. NUMERICAL INSTABILITY IN TSUNAMI SIMULATION 1A

Numerical simulation 1A (average-event tsunami runup scenario) developed a numerical instability in one small area near the mouth of the Siuslaw Estuary. The instability led to anomalously large wave elevations (Figure A23) over several thousand feet of shoreline in the vicinity of North Jetty Road (Figure A24). The point data for maximum wave elevations affected by the instability (file 1A_florence.maxelv.txt, Table 3) were deleted from the ASCII text file within the GIS polygon of Figure A24 (polygon is GIS file Instability and corrected ASCII file is _1A_maxelvNoInstability.txt, Table 3). Data were judged affected if maximum wave elevations showed sharp increases landward that were not seen in the other two

simulations, 2Cs (small-event wave) and 1A + asperity (large-event wave) in the same area.

Numerical instabilities are frequently caused by the geometry and spacing of the numerical grid. Further testing and refinement of the numerical grid could probably remove the instability but was beyond the resources available for the project. The instability did not affect either the 2Cs (small event) or 1A + asperity (large event) simulations using the identical grid; therefore, as the 1A inundation lies at an elevation and lateral extent intermediate between the other two scenarios, it was relatively straightforward to infer the inundation for the 1A simulation within the affected area.

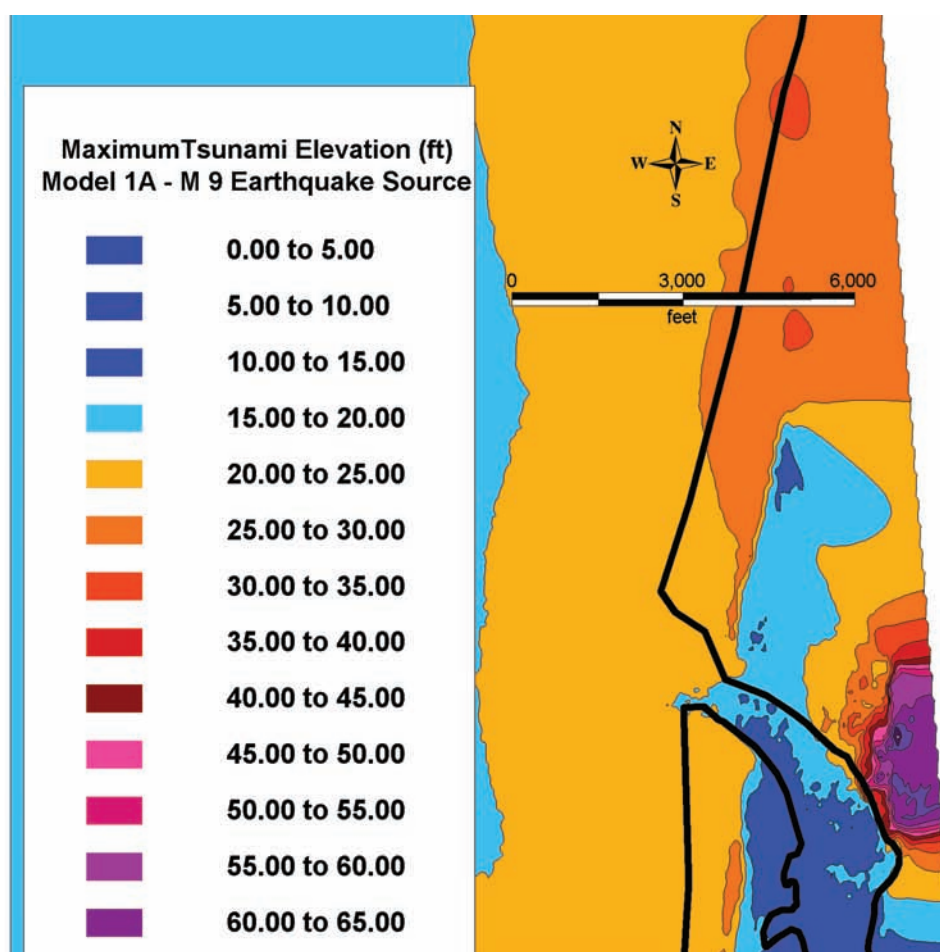


Figure A23. Numerical instability in the 1A simulation generated anomalously high wave elevations in and around the area colored purple on the map. Black line is the approximate shoreline at the mouth of the Siuslaw River; the jetties are not shown.



Figure A24. Location of numerical data deleted from the maximum elevation data file 1A_florence.maxelv.txt for the scenario 1A simulation (average event) to produce file _1A_maxelvNoInstability.txt.